# Accepted Manuscript


Synthesis of α, β-Unsaturated Carbonyl Based Compounds as Acetylcholinesterase and Butyrylcholinesterase Inhibitors: Characterization, Molecular Modeling, QSAR Studies and Effect Against Amyloid β-Induced Cytotoxicity

Syed Nasir Abbas Bukhari, Ibrahim Jantan, Vijay H. Masand, Devidas T. Mahajan, Muhammad Sher, M. Naeem-ul-Hassan, Muhammad Wahab Amjad, Oya Unsal Tan

PII: S0223-5234(14)00553-4

DOI: 10.1016/j.ejmech.2014.06.034

Reference: EJMECH 7077

To appear in: *European Journal of Medicinal Chemistry*

Received Date: 21 February 2014

Revised Date: 12 June 2014

Accepted Date: 17 June 2014

Please cite this article as: S.N.A. Bukhari, I. Jantan, V.H. Masand, D.T. Mahajan, M. Sher, M. Naeem-ul-Hassan, M.W. Amjad, O. Unsal Tan, Synthesis of α, β-Unsaturated Carbonyl Based Compounds as Acetylcholinesterase and Butyrylcholinesterase Inhibitors: Characterization, Molecular Modeling, QSAR Studies and Effect Against Amyloid β-Induced Cytotoxicity, *European Journal of Medicinal Chemistry* (2014), doi: 10.1016/j.ejmech.2014.06.034.

## Graphical Abstract

**Synthesis of α, β-Unsaturated Carbonyl Based Compounds as Acetylcholinesterase and Butyrylcholinesterase Inhibitors: Characterization, Molecular Modeling, QSAR Studies and Effect Against Amyloid β-Induced Cytotoxicity**

Syed Nasir Abbas Bukhari, Ibrahim Jantan, Vijay H. Masand, Devidas T. Mahajan , Muhammad Sher, M.Naeem-ul-Hassan, Muhammad Wahab Amjad, Oya Unsal Tan

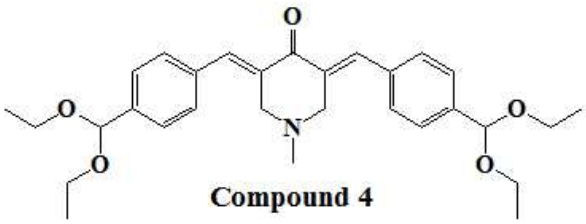


AChE
$IC_{50}$ = 0.042 µM

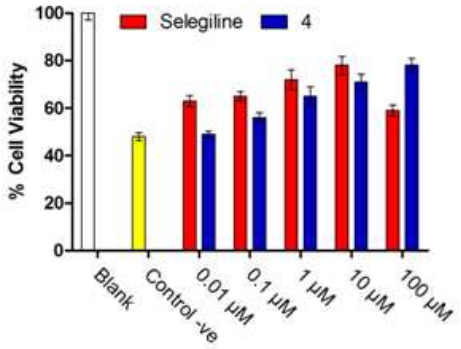


Protective effect of compound **4** against Aβ-induced cytotoxicity

**Synthesis of α, β-Unsaturated Carbonyl Based Compounds as Acetylcholinesterase and Butyrylcholinesterase Inhibitors: Characterization, Molecular Modeling, QSAR Studies and Effect Against Amyloid β-Induced Cytotoxicity**

Syed Nasir Abbas Bukhari, Ibrahim Jantan, Vijay H. Masand, Devidas T. Mahajan, Muhammad Sher, M.Naeem-ul-Hassan, Muhammad Wahab Amjad, Oya Unsal Tan

**Highlights:**

- We synthesized and characterized thirty novel molecules.
- Compound **14** exhibited strong free radical scavenging activity (18.39µM).
- Six compounds showed strong neuroprotective effect.
- Compounds **4** and **14**, containing *N*-methyl-4-piperidone linker, showed high acetylcholinesterase inhibitory activity.

# Synthesis of α, β-Unsaturated Carbonyl Based Compounds as Acetylcholinesterase and Butyrylcholinesterase Inhibitors: Characterization, Molecular Modeling, QSAR Studies and Effect Against Amyloid β-Induced Cytotoxicity

Syed Nasir Abbas Bukhari[a]*, Ibrahim Jantan[a]*, Vijay H. Masand[b], Devidas T. Mahajan[b,] Muhammad Sher[c], M.Naeem-ul-Hassan[c], Muhammad Wahab Amjad[a], Oya Unsal Tan[d]

a. *Drug and Herbal Research Centre, Faculty of Pharmacy, Universiti Kebangsaan Malaysia, Jalan Raja Muda Abdul Aziz, 50300 Kuala Lumpur, Malaysia*
b. *Department of Chemistry, Vidya Bharati Mahavidyalaya, Amravati, Maharashtra, India-444 602.*
c. *Department of Chemistry, University of Sargodha, Sargodha 40100, Pakistan.*
*d*. *Department of Pharmaceutical Chemistry, Faculty of Pharmacy, Hacettepe University, Ankara 06100, Turkey*

***** Authors to whom correspondence should be addressed;

E mail: (SNAB) snab@pharmacy.ukm.my; snab_hussaini@yahoo.com

(IJ) ibj@pharmacy.ukm.my

Tel: +6-01123695295

Fax: +6-0326983271

**ABSTRACT**

A series of novel carbonyl compounds was synthesized by a simple, eco-friendly and efficient method. These compounds were screened for anti-oxidant activity, *in vitro* cytotoxicity and for inhibitory activity for acetylcholinesterase and butyrylcholinesterase. The effect of these compounds against amyloid β-induced cytotoxicity was also investigated. Among them, compound **14** exhibited strong free radical scavenging activity (18.39µM) while six compounds (**1**, **3**, **4**, **13**, **14**, and **19**) were found to be the most protective against Aβ-induced neuronal cell death in PC12 cells. Compounds **4** and **14**, containing *N*-methyl-4-piperidone linker, showed high acetylcholinesterase inhibitory activity as compared to reference drug donepezil. Molecular docking and QSAR (Quantitative Structure-Activity Relationship) studies were also carried out to determine the structural features that are responsible for the acetylcholinesterase and butyrylcholinesterase inhibitory activity.

**KEYWORDS:** Alzheimer's disease, neuroprotection, oxidative stress, 4-piperidone, synthesis.

## 1. INTRODUCTION

According to the World Alzheimer Report 2013, Alzheimer's disease and other forms of dementia are among the biggest global public health issues facing our generation. Currently, over 35 million people around the world live with these conditions and this number is likely to increase threefold by 2050, to 115 million people [1]. Alzheimer's disease (AD), the most common form of dementia amongst the aged, is a deadly neurodegenerative disease categorized by the loss of mental abilities and a diversity of neuropsychiatric symptoms and behavioral disorders [2, 3]. Neurofibrillary tangles and amyloid β (Aβ) plaques are found in the brain. The cholinergic system is predominantly vulnerable to synapse loss, particularly in cortical regions related with memory and executive function [4]. Most treatment approaches to date have been based on the cholinergic hypothesis which assumes that memory loss in patients suffering from this disease result from a loss of cholinergic function in brain for cholinergic neurotransmission is specifically affected in patients suffering from Alzheimer's disease.

For the treatment of AD, one of the most common methods is to increase the acetylcholine levels in brain with acetylcholinesterase inhibitors [5]. The best characterized therapeutic effect of cholinesterase inhibitors (ChE) in Alzheimer disease patients is to maintain cognitive function for a 1-year period in about 50% of the patients [6]. Two kinds of cholinesterase enzymes are found in the central nervous system; acetylcholinesterase (AChE) and butyrylcholinesterase (BuChE). Both enzymes are capable of hydrolyzing acetylcholine, but AChE has a $10^{13}$-fold higher hydrolytic acetylcholine activity than BuChE, at the similar temperature and pH [7]. In the healthy brain, BuChE is thought to play a trivial role in regulating brain acetylcholine levels. In the AD brain, BuChE activity rises while AChE activity remains unchanged or declines. Hence, both enzymes may contribute to regulating acetylcholine levels and are appropriate therapeutic targets to enhance the cholinergic deficit. The two enzymes vary

in location, substrate specificity and kinetics. The most recent studies suggest that BuChE might also have a part in the etiology and development of AD beyond the regulation of synaptic acetylcholine levels. Experimental evidence from the use of agents with improved selectivity for BuChE and ChE, such as rivastigmine (having dual inhibitory action on both AChE and BuChE), shows that there are possible therapeutic benefits of inhibiting both AChE and BuChE in AD and associated dementias. The development of specific small molecule drugs BuChE inhibitors with the capability to inhibit BuChE together with AChE should lead to better clinical outcomes [8].

In our previous studies, we synthesized and screened the series of novel chalcone derivatives and curcumin analogues with α, β-carbonyl linkers for their activity against phagocytic chemotaxis and the production of reactive oxygen species (ROS) from zymosan stimulated human phagocytes. On the basis of these findings and a those of other scientists, it was determined that chalcone derivatives and curcumin-like compounds bearing α, β-carbonyl group have a wide diversity of pharmacological activities [9-14]. Our latest studies showed that a range of compounds with a α, β-unsaturated moiety are capable of inhibiting both AChE and BuChE and can be possible candidates for the treatment of Alzheimer's disease [15, 16].

Numerous studies have documented increased protein oxidation [17] and reactive oxygen species (ROS) formation [18] in the brain tissue of AD patients. Aβ is considered to be a cause of lipid peroxidation in brain cell membranes that may contribute to neurodegeneration [19, 20]. Encouraged by these results, we continued our work in this area, and in the current study we synthesized thirty novel compounds bearing the α, β-carbonyl moiety and have screened them for their effects on the AChE/BuChE activities in addition to amyloid β-Induced cytotoxicity in PC12 cells. Lastly, molecular modeling calculations and QSAR studies were performed to understand the structural basis for the biological activity of compounds.

## 2. RESULTS AND DISCUSSION

### *2.1. Chemistry*

Thirty novel compounds of ten different types were synthesized in the current study as reported previously [21, 22]. To synthesize the desired α, β-unsaturated carbonyl based compounds, Claisen-Schmidt condensation was used [23] between different ketones and suitable aryl aldehydes at a molar ratio 1:2, (twenty one compounds, **1-7**; **11-17**; **21-27**) in the presence of NaOH in ethanol. Some compounds were synthesized in acetic acid in the presence of dry HCl gas. Nine compounds (**8-10**; **18-20**; **28-30**) resembling chalcone analogues were synthesized by same Claisen-Schmidt condensation using molar ratio 1:1 of ketone and aldehyde (Scheme 1). Eight compounds (**7**, **8**, **10**, **17**, **18**, **20**, **27**, **28**) were synthesized using both types of catalytic systems comprising NaOH and the dry HCl gas mixture. As compared to NaOH, the catalytic system with HCl gas mixture produced compounds more efficiently with a higher yield. When using NaOH, a mixture of numerous unidentified products was obtained requiring extensive purification by column chromatography.

All synthesized new compounds were characterized by spectrophotometric techniques as well as elemental analysis of C, H, and N, and melting points. Carbon nuclear magnetic resonance spectra were also obtained. For compounds **3**, **13** and **23**, the NH absorption peaks were not seen in the $^{1}$H NMR spectra of the compounds. Absence of NH absorption peaks is also reported previously by other researchers [24, 25].

### *2.2. Antioxidant activity of α, β-unsaturated carbonyl based compounds*

The DPPH (1,1-diphenyl-1-picrylhydrazyl) assay was performed to assess the compounds for their antioxidant activity. The data of the antioxidant assay is summarized in Table 1. According to the data, five compounds (**1**, **3**, **4, 14** and **19**) were found to possess potent DPPH radical

scavenging activity with $IC_{50}$ in the range of 18.39 to 22.99 µM. Compound **14,** having a *N*-methyl-4-piperidone linker and diethoxymethyl substitution at position 4 of aromatic rings, showed the strongest antioxidant activity (18.39 µM), even more than the positive control (ascorbic acid; 19.36 µM). Among all thirty compounds, only eleven compounds have poor antioxidant activities, exhibiting $IC_{50}$ values greater than 50µM.

*2.3.Cytotoxicity of synthetic compounds in PC12 cells*

To investigate the effect of the new compounds on cell viability, the MTT assay was conducted on PC12 cells. The cells were incubated with varying concentrations (0.01-100 µM) of the test compounds for 24 h and under these conditions the α, β-unsaturated carbonyl based compounds were nontoxic to PC12 cells at any of the concentrations tested.

*2.4.Neuroprotective effect of synthetic compounds against Aβ-induced cell cytotoxicity*

The MTT assay was performed to evaluate the effect of novel synthetic compounds on Aβ-induced PC12 cell toxicity. The cells treated with Aβ exhibited significantly reduced cell viability as compared to control cells (decreased cell viability by 48%). Pretreatment of cells with the synthetic compounds protected against Aβ-induced cell death up to 87%, at a concentration of 100 µM. Six compounds (**1**, **3**, **4**, **13**, **14**, **19**) were the most protective against Aβ-induced PC12 cell toxicity (Figure 1). As compared to the positive control selegiline, the protective effect of the synthetic compounds was significantly higher with compound (**14**) being the best. Amongst the tested compounds, all those possessing 2-nitro and 4-dimethylamine groups (**11-20**) had extremely high protective activities, while a diethoxymethyl group at position 4 of the rings (**1-10**) lead to significantly less protective activity. The presence of pyrolidine at position 4 of compounds (**21-30**) decreased the protective activity against Aβ-induced cytotoxicity. Compounds having a 4-piperidone (**3**, **13**) and those possessing *N*-methyl-4-piperidone (**4**, **14**)

linker exhibited somewhat more protection as compared to all other compounds. These results suggest that a few of the novel α, β-unsaturated carbonyl based compounds may reduce cell damage caused by Aβ-induced cytotoxicity.

*2.5. Acetylcholinesterase and butyrylcholinesterase inhibition activity*

Evaluation of new compounds for their inhibitory effects on AChE and BChE was done by Ellman's method. The screening of novel α, β-unsaturated carbonyl based compounds against AChE and BChE demonstrated that nearly all these were moderate to strongly active against AChE (Table 1). The compounds were found to be less active on BChE but most inhibited AChE to various extents. The $IC_{50}$ values of the compounds **8, 9, 15-18, 21, 22, 25, 26,** and **28-30** could not be calculated owing to their weak inhibition potency, which did not surpass 50% at the highest concentration (100 μM). In contrast, the compounds **3**, **4**, **12-14**, **23** and **24** exhibited $IC_{50}$ values ranging from 0.042 to 9.52 μM for inhibition of AChE. In addition, the compounds **3**, **4**, **13** and **14** showed substantial AChE inhibitory activity below 1μM, which is similar to that of donepezil (0.062μM). The compounds **4** and **14**, having *N*-methyl-4-piperidone linker, had a better inhibitory potency than the reference drug donepezil. For the inhibition of BuChE, compounds **3**, **7** and **12** displayed $IC_{50}$ below 20μM, but none was found more active than donepezil (6.92 μM).

These findings encouraged us to explore the relationship between AChE inhibitory activity and the chemical structures of the compounds. Ten varying types of ketones were used as linkers, but only three types of linkers present in compounds (**3**, **4**, **12**, **13**, **14**, **23**, and **24**) were found to be the most effective. The presence of tetrahydropyran-4-one linker displayed good inhibition but only in the presence of 2-nitro and 4-dimethylamine substitution patterns (Compound **12**). Table 1 shows that the compounds (**4**, **14**, and **24**) having *N*-methyl-4-piperidone linker were strong

inhibitors of AChE. Synthetic α, β-unsaturated carbonyl based compounds possessing the 4-piperidone moiety (**3**, **13,** and **23**) were also good inhibitors but relatively weaker than those with 4-piperidone linker. In an earlier study, Yalda et al. reported the synthesis of piperidone-grafted novel mono- and bisspiro heterocyclic hybrids containing functionalized piperidine, pyrrolizine and oxindole rings. The cholinesterase inhibitory activity of those cycloadducts revealed that monospiripyrrolizines were more active with $IC_{50}$ in the range of 3.36 to 20.07 µM than dipolarophiles or bisspiropyrrolizines [26]. The current investigation shows that the increased activity is the result of specific linkers, whereas substitution patterns on the linked aromatic rings participated to lesser extent. The comparison amongst the three active compounds with same linker (**4**, **14**, **24**) revealed that compound **4** with diethoxymethyl group at position 4 of the aromatic rings showed more activity than compound **14** possessing a 2-nitro and 4-dimethylamine substitution pattern. The introduction of pyrrolidine at position 4 of compound **24** reduced the inhibition of AChE. A similar like activity relationship was also observed amongst compounds (**3**, **13** and **23**), having 4-piperidone groups on the aromatic rings. The activities of these compounds showed that the linkers derived from ketones during synthesis play key roles in terms of inhibitory activity. Compounds (**1-10**) have similar substitution pattern, but only two compounds (**3**, **4**) with 4-piperidone and *N*-methyl-4-piperidone moieties are potent inhibitors. Similar results were seen amongst other two series of synthetic compounds (**11-20** and **21-30**). Contreras et al. reported the synthesis of novel compounds by using 1-benzyl-4-piperidone and a conventional structure-activity relationship examination proposed that the presence of a central pyridazine ring is vital for high AChE inhibition [27]. The data in our current investigation support the significance of the piperidone moiety for the inhibition of AChE.

*2.6. Docking and QSAR analyses*

Molecular docking analysis was performed to obtain better insight into mechanism of action of the AChE inhibitors. The active site of AChE is located at the base of ~20A$^{o}$ deep and narrow gorge, from the surface of the enzyme and is composed by two subsites [28, 29]: (1) catalytic esteratic site (CES) and (2) peripheral anionic site (PAS). The active site consists of Gln71-Tyr-Val-Asp-Thr-Leu76, Gly82-Thr-Glu84, Trp86-Asn-Pro88, Tyr121, Leu130, Tyr133, Glu199, Ser200, Glu202-Ser-Ala204, Trp279, Trp286, Phe295, Phe297, Glu327, Phe330, Tyr334, Tyr337-Phe338, Tyr341, Trp439, His447-Gly-Tyr449, and Ile451. The mechanism of acetylcholine (ACh) hydrolysis involves trapping of ACh to PAS, followed by the transfer of ACh to the active site.

[Insert figure 2 and 3 here]

From figure 2 and 3, it is clear that the most active AChE inhibitor (Compound **4)** interacts with the receptor mainly due to hydrophobic and mild polar interactions. The close proximity of compound **4** with Tyr334 and Trp279 is due to mild polar interactions, indicating that it binds reversibly with the receptor.

QSAR analysis: For QSAR analysis, a myriad number of descriptors were calculated followed by elimination of redundant descriptors using QSARINS. Then, GA-MLR (Genetic Algorithm-Multilinear Regression) was performed to develop robust QSAR model. The best two parametric QSAR model along with its statistical parameters is as following:

$pIC_{50}$ = 126.3811 (±28.0863) -7.2606 (±2.3866) RDF090m -4.8896 (±2.0119) F01[C-N]

$N_{tr}$ = 14, $N_{ex}$ = 3, $R^2$ = 0.8558, $R^2_{adj}$ = 0.8296, $CCC_{tr}$ = 0.9223, F = 32.6359, $Q^2_{LOO}$ = 0.7924, $CCC_{cv}$ = 0.8897, $R^2_{ex}$ = 0.7718, $CCC_{ex}$ = 0.8578

The symbols have the usual meaning [30-33]. The high value of $R^2$, $R^2$adj, $CCC_{tr}$, F, $Q^2_{LOO}$, $CCC_{cv}$ and $R^2_{ex}$ indicates that the QSAR model is not only robust but also possesses good predictive ability [30-35]. Since the model is based on a data set of seventeen molecules only, further improvements in the external predictive ability are also possible. From the QSAR model, it is clear that activity has correlation with RDF090m (Radial Distribution Function - 9.0 / weighted by atomic masses, RDF descriptors) and F01[C-N] (frequency of C - N at topological distance of 01, a 2D frequency fingerprints descriptor). It is quite clear that the docking and the QSAR analyses not only support each other but are complementary to each other also.

## 3. CONCLUSION

In the work described above, we report the synthesis, pharmacological evaluation and molecular modeling of thirty novel α, β-unsaturated carbonyl based compounds. From docking and QSAR analyses, it can be stated that lipophilicity steers the AChE activity which is additionally supported by the hydrophobic interactions between the ligand and the receptor. We propose that the free radical scavenging activity of these novel compounds is responsible for their neuroprotective effects as it was seen that all strong antioxidant compounds possess more protective effect against Aβ-induced PC12 cell death. The most potent AChE inhibitors in this series correspond to *N*-methyl-4-piperidone and 4-piperidone moieties. The type of the substituent at the aromatic rings in compounds does not appear to have a strong influence on the inhibitory activity. Overall, the substitution of benzene rings by diethoxymethyl group at position 4 and presence of piperidone moiety imparts strong acetylcholinesterase inhibition. The multiple

activities of these compounds suggest that they may be useful for the treatment of neurodegenerative diseases such as AD that involve a loss of cholinergic neurons.

## 4. Experimental

### *4.1.Materials*

All chemicals and reagents were purchased from Sigma-Aldrich, Merck and Acros Organics (above 98% purity) and were used without additional purification. MTT [3-(4,5-dimethylthiazol-2-yl)-2,5-diphenyltetrazolium bromide] was procured from Sigma-Aldrich (St. Louis, MO, USA). AChE, (E.C.3.1.1.7 from Electric Eel, 500 units), BChE, (E.C. 3.1.1.8, from horse serum, 1000 units) and donepezil hydrochloride were also purchased from Sigma–Aldrich. $A\beta_{1-42}$ was purchased from Bachem (Bubendorf, Switzerland). Potassium dihydrogen phosphate, 5,5'-dithiobis-(2-nitrobenzoic acid (DTNB), potassium hydroxide, sodium hydrogen carbonate, gelatine, acetylthiocholine iodide (ATC) and butrylthiocholine iodide (BTC) were supplied by Fluka (Buchs, Switzerland). Spectrophotometric analyses were performed using a Shimadzu UV-1700, UV–Vis spectrophotometer. Phosphate buffer (100mM, pH 8.0) at 25°C was used to measure cholinesterase activity of the compounds, using ATC and BTC (75 mM) as substrates. In both cases, DTNB (10 mM) was used to observe absorbance changes at 412 nm. Donepezil hydrochloride was used as a positive control [36].

### *4.2.General Procedures*

$^{1}H$ and $^{13}C$ NMR spectra were recorded on a JEOL ECP spectrometer operating at 500 MHz, with Me4Si as internal standard and $CDCl_3$ or DMSO-$d^6$ as the solvent. Electrospray ionization mass spectrometry (ESI-MS) on MicroTOF-Q mass spectrometer (Bruker) was used to obtain high resolution mass spectra (HRMS). Microanalyses data was obtained using Fison EA 1108

elemental analyzer. Infrared spectra using KBr disc were recorded on a Perkin Elmer 400 (FTIR) spectrometer. Flash column chromatography was carried out with silica gel 60 (230-400mesh) (Merck) and thin layer chromatography (TLC) was performed on pre-coated silica plates (kiesel gel 60 $F_{254}$, BDH). Melting points were determined using an electrothermal instrument and are uncorrected. The compounds were visualized by illumination under ultraviolet (UV) light (254 nm) or by vanillin stain followed by charring on a hotplate.

*4.3.Synthesis of α, β-Unsaturated Carbonyl based Compounds*

Twenty one α, β-unsaturated carbonyl based compounds (**1-7**; **11-17**; **21-27**) were synthesized by direct coupling of the appropriate aromatic aldehyde with the ten different types of ketones at a molar ratio of 1:2, and the compounds (**8-10**; **18-20**; **28-30**) were synthesized at a molar ratio of 1:1 under base catalyzed Claisen–Schmidt condensation reaction conditions. Scheme 1 demonstrates the general synthesis of α, β-unsaturated carbonyl based compounds d. Concisely, the appropriate aromatic aldehyde (20 mmol, 2 equivalant) and the suitable ketone (10 mmol, 1 equivalent) were mixed and dissolved in 15 mL of ethanol in single necked round bottomed flask, and stirred at 5°C for a couple of minutes. Afterwards, a 40% NaOH solution in ethanol was then added drop wise for several minutes. The mixture was left stirring at room temperature (27 °C) for 1-24 h. The precipitate formation and color changes of the reaction mixture served as an indication of product formation. The reaction was monitored by TLC and upon completion; the reaction was quenched by the addition of acidified ice to the mixture. The α, β-unsaturated carbonyl based compounds were isolated by column chromatography or by recrystallization.

*4.3.1. 2,6-Bis[4-(diethoxymethyl)benzylidene]cyclohexanone* (**1**)

Yellow crystals (2.59 g, 54%). mp: 112-114 ˚C; $^{1}$H NMR (500 MHz, $CDCl_3$) δ: 7.89 (s, 2H), 7.29 (d, J=8Hz, 4H), 6.82 (d, J=8Hz, 4H), 5.89 (s, 2H), 3.42 (q, J=7.5, 8H), 2.32 (t, J=12.0 Hz, 4H), 1.82 (m, 2H), 1.24 (t, J=7.5, 12H); $^{13}$C NMR (500 MHz, $CDCl_3$) δ: 186.4, 152.9, 144.4, 136.5, 132.5, 127.3, 126.5, 101.1, 55.0, 28.3, 27.8, 16.2 ; HRMS (ESI) m/z: 479.68 $[M+H]^+$, Microanalysis calculated for $C_{30}H_{38}O_5$ (478.62), C: 75.28%, H: 8.00%. Found C: 75.42%, H: 8.12%.

*4.3.2. 3,5-Bis-(4-diethoxymethyl-benzylidene)-tetrahydro-pyran-4-one* (**2**)

Pale Yellow crystals (3.06 g, 64%). mp: 106-108 ˚C; $^{1}$H NMR (500 MHz, $CDCl_3$) δ: 7.85 (s, 2H), 7.32 (d, J=8Hz, 4H), 6.95 (d, J=8Hz, 4H), 5.52 (s, 2H), 3.62 (q, J=7.5, 8H), 2.69 (s, 4H), 1.18 (t, J=8, 12H); $^{13}$C NMR (500 MHz, $CDCl_3$) δ: 187.2, 152.7, 143.8, 136.7, 131.9, 126.2, 125.2, 101.5, 62.4, 55.2, 16.1; HRMS (ESI) m/z: 481.65 $[M+H]^+$, Microanalysis calculated for $C_{29}H_{36}O_6$ (480.59), C: 72.48%, H: 7.55%. Found C: 72.62%, H: 7.72%.

*4.3.3. 3,5-Bis[4-(diethoxymethyl)benzylidene]piperidin-4-one* (**3**)

Yellow solid (2.89 g, 60%). mp: 101-102 ˚C; $^{1}$H NMR (500 MHz, $CDCl_3$) δ: 7.68 (s, 2H), 7.12 (d, J=7.5Hz, 4H), 6.93 (d, J=7.5Hz, 4H), 5.65 (s, 2H), 3.36 (q, J=7.5, 8H), 2.65 (s, 4H), 1.27 (t, J=7.0, 12H); $^{13}$C NMR (500 MHz, $CDCl_3$) δ: 185.2, 145.1, 144.5, 138.5, 136.2, 128.1, 127.8, 102.1, 55.1, 48.7, 16.4 ; HRMS (ESI) m/z: 480.71 $[M+H]^+$, Microanalysis calculated for $C_{29}H_{37}NO_5$ (479.61), C: 72.62%, H: 7.78%, N: 2.92%. Found C: 72.71%, H: 7.86%, N: 3.10%.

*4.3.4. 3,5-Bis[4-(diethoxymethyl)benzylidene]-1-methyl-piperidin-4-one* (**4**)

Light Yellow solid (2.12 g, 43%). mp: 142-144 ˚C; $^{1}$H NMR (500 MHz, $CDCl_3$) δ: 7.63 (s, 2H), 7.32 (d, J=8Hz, 4H), 7.15 (d, J=8Hz, 4H), 5.59 (s, 2H), 3.29 (q, J=7.5, 8H), 2.71 (s, 4H), 2.12 (s, 3H), 1.20 (t, J=7.0, 12H); $^{13}$C NMR (500 MHz, $CDCl_3$) δ: 189.7, 148.2, 147.5, 139.8, 135.1, 128.4, 127.1, 101.4, 56.6, 51.2, 40.1, 16.7 ; HRMS (ESI) m/z: 494.65 $[M+H]^+$, Microanalysis calculated for $C_{30}H_{39}NO_5$ (493.63), C: 72.99%, H: 7.96%, N: 2.84%. Found C: 72.95%, H: 7.99%, N: 2.87%.

*4.3.5. 1-Benzyl-3,5-bis[4-(diethoxymethyl)benzylidene]piperidin-4-one* (**5**)

Brown semisolid (2.76 g, 48%). mp: 112-114 ˚C; $^{1}$H NMR (500 MHz, $CDCl_3$) δ: 7.89 (d, J=8Hz, 2H), 7.65 (s, 2H), 7.52 (d, J=8Hz, 2H), 7.22 (d, J=7Hz, 4H), 7.12 (d, J=7Hz, 4H), 6.69 (t, J=6.5Hz, H), 5.17 (s, 2H), 4.17 (s, 2H), 3.38 (q, J=7.5Hz, 8H), 2.95 (s, 4H), 1.14 (t, J=7.0, 12H); $^{13}$C NMR (500 MHz, $CDCl_3$) δ: 191.5, 148.2, 147.9, 139.5, 139.1, 132.5, 128.4, 127.6, 127.0, 125.2, 124.9, 101.8, 64.3, 56.2, 50.92, 17.1 ; HRMS (ESI) m/z: 570.84 $[M+H]^+$, Microanalysis calculated for $C_{36}H_{43}NO_5$ (569.73), C: 75.89%, H: 7.61%, N: 2.46%. Found C: 75.92%, H: 7.64%, N: 2.44%.

*4.3.6. 1,5-Bis-(4-diethoxymethyl-phenyl)-penta-1,4-dien-3-one* (**6**)

Pale brownish solid (1.96 g, 45%). mp: 98-100 ˚C; $^{1}$H NMR (500 MHz, $CDCl_3$) δ: 7.82 (d, J=6.5Hz, 4H), 7.71 (d, J=8Hz, 2H) , 7.49 (d, J=6.5Hz, 2H), 7.16 (d, J=7Hz, 4H), 5.25 (s, 2H), 3.52 (q, J=7Hz, 8H), 1.17 (t, J=7.0, 12H); $^{13}$C NMR (500 MHz, $CDCl_3$) δ: 190.5, 152.2, 148.6, 139.7, 136.4, 135.2, 132.8, 102.2, 55.5, 16.9 ; HRMS (ESI) m/z: 439.62 $[M+H]^+$, Microanalysis calculated for $C_{27}H_{34}O_5$ (438.56), C: 73.94%, H: 7.81%. Found C: 74.12%, H: 7.89%.

*4.3.7. 2,5-Bis-(4-diethoxymethyl-benzylidene)-cyclopentanone* (**7**)

Light yellow crystals (3.12 g, 67%). mp: 88-89 ˚C; $^{1}$H NMR (500 MHz, $CDCl_3$) δ: 7.69 (d, J=6.5Hz, 4H), 7.42 (s, 2H), 7.21 (d, J=6.5Hz, 4H), 5.45 (s, 2H), 3.62 (q, J=7Hz, 8H), 2.38 (t, J=7Hz, 4H), 1.22 (t, J=7.0, 12H); $^{13}$C NMR (500 MHz, $CDCl_3$) δ: 189.7, 149.4, 145.5, 138.7, 136.4, 133.9, 129.1, 100.9, 56.2, 32.5, 16.1 ; HRMS (ESI) m/z: 465.72 $[M+H]^+$, Microanalysis calculated for $C_{29}H_{36}O_5$ (464.59), C: 74.97%, H: 7.81%. Found C: 75.18%, H: 7.87%.

*4.3.8. 2-(4-Diethoxymethyl-benzylidene)-indan-1-one* (**8**)

White powder (2.52 g, 78%). mp: 152-154 ˚C; $^{1}$H NMR (500 MHz, $CDCl_3$) δ: 7.80 (d, J=8Hz, 2H), 7.69 (s, H), 7.48 (d, J=8Hz, 2H), 7.25 (d, J=7.5Hz, H), 7.20 (d, J=7.5Hz, H), 7.05 (t, J=7.5Hz, H), 6.94 (t, J=7Hz, H), 5.34 (s, H), 3.49 (q, J=7Hz, 4H), 2.75 (s, 2H), 1.29 (t, J=6Hz, 6H); $^{13}$C NMR (500 MHz, $CDCl_3$) δ: 193.2, 144.5, 142.2, 140.1, 139.2, 138.8, 136.5, 130.4, 129.6, 128.1, 125.6, 125.1, 124.2, 102.2, 56.3, 29.9, 16.4 ; HRMS (ESI) m/z: 323.67 $[M+H]^+$, Microanalysis calculated for $C_{21}H_{22}O_3$ (322.40), C: 78.23%, H: 6.88%. Found C: 78.44%, H: 6.92%.

*4.3.9. 2-(4-Diethoxymethyl-benzylidene)-3,4-dihydro-2H-naphthalen-1-one* (**9**)

Light yellow solid (2.67g, 80%). mp: 94-95 ˚C; $^{1}$H NMR (500 MHz, $CDCl_3$) δ: 7.84 (d, J=8Hz, 2H), 7.59 (s, H), 7.47 (d, J=8.5Hz, 2H), 7.29 (d, J=7.5Hz, H), 7.22 (d, J=7.5Hz, H), 7.12 (t, J=7.5Hz, H), 7.02 (t, J=7Hz, H), 5.49 (s, H), 3.35 (q, J=7Hz, 4H), 2.29 (t, J=7Hz, 2H), 2.05 (t, J=7Hz, 2H), 1.17 (t, J=6Hz, 6H); $^{13}$C NMR (500 MHz, $CDCl_3$) δ: 188.3, 152.2, 150.1, 148.5, 146.2, 143.9, 137.5, 134.4, 129.2, 127.2, 126.2, 124.8, 117.2, 101.7, 56.2, 29.5, 28.2, 16.0 ; HRMS (ESI) m/z: 337.51 $[M+H]^+$, Microanalysis calculated for $C_{22}H_{24}O_3$ (336.42), C: 78.54%, H: 7.19%. Found C: 78.33%, H: 7.12%.

*4.3.10. 2-[3-(4-Diethoxymethyl-phenyl)-acryloyl]-3,4-dihydro-2H-naphthalen-1-one* (**10**)

Yellow solid (3.16 g, 83%). mp: 121-122 ˚C; $^{1}$H NMR (500 MHz, $CDCl_3$) δ: 7.75 (d, J=6Hz, H), 7.52 (d, J=6Hz, H), 7.42 (d, J=8Hz, 2H), 7.39 (d, J=8Hz, 2H), 7.32 (d, J=7Hz, H), 7.29 (d, J=7Hz, H), 7.17 (t, J=7Hz, H), 6.89 (t, J=7Hz, H), 5.29 (s, H), 3.47 (q, J=7Hz, 4H), 3.29 (t, J=8.5Hz, H), 2.12 (t, J=8Hz, 2H), 1.95 (t, J=7Hz, 2H), 1.24 (t, J=6.5Hz, 6H); $^{13}$C NMR (500 MHz, $CDCl_3$) δ: 194.6, 151.1, 148.9, 144.6, 142.3, 139.2, 138.4, 136.2, 135.5, 132.4, 130.6, 129.1, 125.2, 124.2, 103.1, 66.1, 55.7, 30.2, 28.6, 16.7 ; HRMS (ESI) m/z: 379.52 $[M+H]^+$, Microanalysis calculated for $C_{24}H_{26}O_4$ (378.46), C: 76.17%, H: 6.92%. Found C: 76.21%, H: 6.91%.

*4.3.11. 2,6-Bis-(4-dimethylamino-2-nitro-benzylidene)-cyclohexanone* (**11**)

White powder (2.78 g, 62%). mp: 139-140 ˚C; δ: 7.94 (s, 2H), 7.55 (d, J=8Hz, 2H), 7.41 (d, J=8Hz, 2H), 7.13 (s, 2H), 3.15 (s, 12H), 2.35 (t, J=12.0 Hz, 4H), 1.87 (m, 2H) ; $^{13}$C NMR (500 MHz, $CDCl_3$) δ: 190.7, 149.5, 145.7, 145.6, 140.1, 128.2, 118.6, 117.6, 106.5, 46.8, 29.1, 27.5; HRMS (ESI) m/z: 451.64 $[M+H]^+$, Microanalysis calculated for $C_{24}H_{26}N_4O_5$ (450.49), C: 63.99%, H: 5.82%, N: 12.44%. Found C: 64.12%, H: 5.72%, N: 12.42%.

*4.3.12. 3,5-Bis[4-(dimethylamino)2-nitro-benzylidene]tetrahydro-pyran-4-one* (**12**)

White powder (2.92 g, 65%). mp: 188- 190 ˚C; $^{1}$H NMR (500 MHz, $CDCl_3$) δ: 7.89 (s, 2H), 7.46 (d, J=8Hz, 2H), 7.14 (d, J=8Hz, 2H), 7.05 (s, 2H), 3.13 (s, 12H), 2.93 (s, 4H); $^{13}$C NMR (500 MHz, $CDCl_3$) δ: 190.5, 149.2, 146.9, 145.1, 139.9, 128.4, 118.9, 118.1, 107.8, 65.5, 46.2; HRMS (ESI) m/z: 475.52 $[M+Na]^+$, Microanalysis calculated for $C_{23}H_{24}N_4O_6$ (452.46), C: 61.05%, H: 5.35%, N: 12.38%. Found C: 61.24%, H: 5.59%, N: 12.42%.

*4.3.13. 3,5-Bis[4-(dimethylamino)2-nitro-benzylidene]piperidin-4-one* (**13**)

Light yellow solid (2.28 g, 51%). mp: 192- 194 ˚C; $^{1}$H NMR (500 MHz, $CDCl_3$) δ: 7.82 (s, 2H), 7.72 (d, J=8Hz, 2H), 7.21 (d, J=8Hz, 2H), 6.92 (s, 2H), 3.17 (s, 12H), 3.13 (s, 4H); $^{13}$C NMR (500 MHz, $CDCl_3$) δ: 189.4, 149.7, 148.6, 142.5, 140.7, 127.3, 118.8, 118.1, 106.5, 49.4, 46.9; HRMS (ESI) m/z: 452.52 $[M+H]^+$, Microanalysis calculated for $C_{23}H_{25}N_5O_5$ (451.48), C: 61.19%, H: 5.58%, N: 15.51%. Found C: 61.42%, H: 5.62%, N: 15.89%.

*4.3.14. 3,5-Bis[4-(dimethylamino)2-nitro-benzylidene]-1-methyl-piperidin-4-one* (**14**)

White powder (2.56 g, 55%). mp: 181- 182 ˚C; $^{1}$H NMR (500 MHz, $CDCl_3$) δ: 7.76 (s, 2H), 7.45 (d, J=8Hz, 2H), 7.23 (d, J=8Hz, 2H), 7.13 (s, 2H), 3.21 (s, 12H), 3.03 (s, 4H), 2.19 (s, 3H); $^{13}$C NMR (500 MHz, $CDCl_3$) δ: 187.5, 148.9, 148.2, 143.2, 141.8, 126.7, 119.6, 118.9, 106.2, 44.5, 46.1, 38.8; HRMS (ESI) m/z: 466.72 $[M+H]^+$, Microanalysis calculated for $C_{24}H_{27}N_5O_5$ (465.50), C: 61.92%, H: 5.85%, N: 15.04%. Found C: 61.99%, H: 5.91%, N: 15.19%.

*4.3.15. 1-Benzyl-3,5-bis-(4-dimethylamino-2-nitro-benzylidene)-piperidin-4-one* (**15**)

White crystals (3.22 g, 60%). mp: 165-166 ˚C; $^{1}$H NMR (500 MHz, $CDCl_3$) δ: 7.82 (d, J=8Hz, 2H), 7.72 (s, 2H), 7.59 (d, J=8Hz, 2H), 7.32 (d, J=7Hz, 2H), 7.25 (t, J=7Hz, 2H), 7.02 (s, 2H), 6.92 (t, J=6.5Hz, H), 4.22 (s, 2H), 3.19 (s, 12H), 2.72 (s, 4H), ; $^{13}$C NMR (500 MHz, $CDCl_3$) δ: 189.6, 148.9, 147.2, 139.5, 139.0, 131.9, 128.6, 126.5, 126.0, 125.3, 124.5, 119.2, 104.9, 64.8, 53.8, 45.9; HRMS (ESI) m/z: 542.65 $[M+H]^+$, Microanalysis calculated for $C_{30}H_{31}N_5O_5$ (541.60), C: 66.53%, H: 5.77%, N: 12.93%. Found C: 66.48%, H: 5.79%, N: 12.54%.

*4.3.16. 1,5-Bis-(4-dimethylamino-2-nitro-phenyl)-penta-1,4-dien-3-one* (**16**)

Pale yellow solid (2.97 g, 68%). mp: 177-179 ˚C; $^{1}$H NMR (500 MHz, $CDCl_3$) δ: 7.70 (d, J=6Hz, 2H), 7.68 (d, J=8Hz, 2H), 7.44 (d, J=6Hz, 2H), 7.25 (d, J=8Hz, 2H), 7.12 (s, 2H), 3.15 (s, 12H);

$^{13}$C NMR (500 MHz, $CDCl_3$) δ: 187.5, 150.9, 148.6, 144.4, 132.8, 128.1, 117.5, 113.8, 107.9, 46.7; HRMS (ESI) m/z: 409.45 $[M-H]^+$, Microanalysis calculated for $C_{21}H_{22}N_4O_5$ (410.42), C: 61.45%, H: 5.40%, N: 13.65%. Found C: 61.48%, H: 5.62%, N: 13.77%.

*4.3.17. 2,5-Bis-(4-dimethylamino-2-nitro-benzylidene)-cyclopentanone* (**17**)

White powder (2.41 g, 55%). mp: 156-157 ˚C; $^1$H NMR (500 MHz, $CDCl_3$) δ: 7.92 (d, J=6.5Hz, 2H), 7.88 (d, J=6Hz, 2H), 7.75 (d, J=6.5Hz, 2H), 7.44 (s, 2H), 3.10 (s, 12H), 2.45 (t, J=7Hz, 4H) ; $^{13}$C NMR (500 MHz, $CDCl_3$) δ: 188.9, 153.2, 149.9, 144.2, 143.8, 125.8, 118.1, 116.4, 108.3, 46.9, 32.6; HRMS (ESI) m/z: 437.72 $[M+H]^+$, Microanalysis calculated for $C_{23}H_{24}N_4O_5$ (436.46), C: 63.29%, H: 5.54%, N: 12.84%. Found C: 63.42%, H: 5.48%, N: 12.72%.

*4.3.18. 2-(4-Dimethylamino-2-nitro-benzylidene)-indan-1-one* (**18**)

Yellow semisolid (1.95 g, 63%). mp: 169-171 ˚C; $^1$H NMR (500 MHz, $CDCl_3$) δ: 7.56 (d, J=8Hz, H), 7.48 (s, H), 7.32 (d, J=8Hz, H), 7.12 (s, H), 6.98 (d, J=7.5Hz, H), 6.91 (d, J=7.5Hz, H), 6.74 (t, J=7.5Hz, H), 6.65 (t, J=7Hz, H), 3.22 (s, 6H), 2.81 (s, 2H); $^{13}$C NMR (500 MHz, $CDCl_3$) δ: 192.8, 145.6, 142.6, 141.3, 139.8, 138.2, 137.4, 130.9, 128.7, 128.0, 125.9, 123.8, 119.5, 117.6, 108.6, 46.8, 28.3 ; HRMS (ESI) m/z: 309.55 $[M+H]^+$, Microanalysis calculated for $C_{18}H_{16}N_2O_3$ (308.33), C: 70.12%, H: 5.23%, N: 9.09%. Found C: 70.18%, H: 5.59%, N: 9.18%.

*4.3.19. 2-(4-Dimethylamino-2-nitro-benzylidene)-3,4-dihydro-2H-naphthalen-1-one* (**19**)

White powder (2.50 g, 78%). mp: 138-139 ˚C; $^1$H NMR (500 MHz, $CDCl_3$) δ: 7.82 (d, J=6.5Hz, H), 7.57 (s, H), 7.42 (d, J=6.5Hz, H), 7.35 (s, H), 7.28 (d, J=7Hz, H), 7.20 (d, J=7Hz, H), 7.19 (t, J=7.5Hz, H), 6.92 (t, J=8Hz, H), 3.14 (s, 6H), 2.47 (t, J=7Hz, 2H), 2.14 (t, J=7Hz, 2H) ; $^{13}$C NMR (500 MHz, $CDCl_3$) δ: 188.7, 152.8, 151.3, 148.9, 146.8, 144.2, 136.8, 134.6, 129.9, 127.6,

126.1, 125.3, 124.2, 107.8, 46.2, 29.9, 27.9; HRMS (ESI) m/z: 323.45 $[M+H]^+$, Microanalysis calculated for $C_{19}H_{18}N_2O_3$ (322.36), C: 70.79%, H: 5.63%, N: 8.69%. Found C: 71.12%, H: 5.52%, N: 8.72%.

*4.3.20. 2-[3-(4-Dimethylamino-2-nitro-phenyl)-acryloyl]-3,4-dihydro-2H-naphthalen-1-one* (**20**)

Pale yellow powder (2.93 g, 80%). mp: 102-103 ˚C; $^1$H NMR (500 MHz, $CDCl_3$) δ: 7.79 (d, J=6.5Hz, H), 7.62 (d, J=6.5Hz, H), 7.45 (d, J=7.5Hz, H), 7.32 (s, H), 7.29 (d, J=7.5Hz, H), 7.21 (d, J=7.5Hz, H), 7.14 (d, J=7.5Hz, H), 7.02 (t, J=7.5Hz, H), 6.94 (t, J=7.5Hz, H), 3.45 (t, J=8.5Hz, H), 3.10 (s, 6H), 2.22 (t, J=8Hz, 2H), 2.15 (t, J=8Hz, 2H) ; $^{13}$C NMR (500 MHz, $CDCl_3$) δ: 193.8, 152.2, 148.7, 145.2, 142.8, 139.6, 137.1, 136.8, 135.6, 131.9, 130.5, 129.4, 124.8, 123.5, 116.5, 106.2, 65.8, 46.8, 31.3, 28.7 ; HRMS (ESI) m/z: 365.55 $[M+H]^+$, Microanalysis calculated for $C_{21}H_{20}N_2O_4$ (364.39), C: 69.22%, H: 5.53%, N: 7.69%. Found C: 69.34%, H: 5.59%, N: 7.81%.

*4.3.21. 2,6-Bis-(4-pyrrolidin-1-yl-benzylidene)-cyclohexanone* (**21**)

Brownish powder (3.12 g, 76%). mp: 105-107 ˚C; $^1$H NMR (500 MHz, $CDCl_3$) δ: 7.92 (s, 2H), 7.45 (d, J=8Hz, 4H), 6.99 (d, J=8Hz, 4H), 2.37 (t, J=10.0 Hz, 4H), 2.10 (m, J=6.5Hz, 8H), 1.84 (m, J=5.5, 2H), ; $^{13}$C NMR (500 MHz, $CDCl_3$) δ: 188.9, 152.2, 145.2, 136.7, 131.9, 127.5, 126.9, 58.1, 28.8, 27.2, 25.6 ; HRMS (ESI) m/z: 413.62 $[M+H]^+$, Microanalysis calculated for $C_{28}H_{32}N_2O$ (412.57), C: 81.51%, H: 7.82%, N: 6.79%. Found C: 81.67%, H: 7.99%, N: 6.95%.

*4.3.22. 3,5-Bis-(4-pyrrolidin-1-yl-benzylidene)-tetrahydro-pyran-4-one* (**22**)

Light Brown solid (2.40 g, 58%). mp: 99-101 ˚C; $^{1}$H NMR (500 MHz, $CDCl_3$) δ: 7.81 (s, 2H), 7.37 (d, J=6.5Hz, 4H), 7.17 (d, J=6.5Hz, 4H), 2.94 (s, 4H), 1.92 (m, J=6.5Hz, 8H) ; $^{13}$C NMR (500 MHz, $CDCl_3$) δ: 189.0, 150.3, 144.7, 136.8, 130.1, 126.8, 125.6, 62.9, 57.1, 25.5; HRMS (ESI) m/z: 415.49 $[M+H]^+$, Microanalysis calculated for $C_{27}H_{30}N_2O_2$ (414.54), C: 78.23%, H: 7.29%, N: 6.76%. Found C: 78.45%, H: 7.52%, N: 6.72%.

*4.3.23. 3,5-Bis-(4-pyrrolidin-1-yl-benzylidene)-piperidin-4-one* (**23**)

Pale yellow powder (2.83 g, 69%). mp: 92-93 ˚C; $^{1}$H NMR (500 MHz, $CDCl_3$) δ: 7.72 (s, 2H), 7.17 (d, J=7.5Hz, 4H), 6.81 (d, J=7.5Hz, 4H), 2.88 (s, 4H), 1.74 (m, J=6Hz, 8H) ; $^{13}$C NMR (500 MHz, $CDCl_3$) δ: 185.7, 145.9, 143.4, 137.1, 136.5, 128.7, 119.9, 56.4, 48.2, 24.9; HRMS (ESI) m/z: 436.62 $[M+Na]^+$, Microanalysis calculated for $C_{27}H_{31}N_3O$ (413.55), C: 78.42%, H: 7.56%, N: 10.16%. Found C: 78.44%, H: 7.60%, N: 10.25%.

*4.3.24. 1-Methyl-3,5-bis[4-(pyrrolidinyl)benzylidene]piperidin-4-one* (**24**)

Yellow powder (1.99 g, 47%). mp: 122- 124 ˚C; $^{1}$H NMR (500 MHz, $CDCl_3$) δ: 7.89 (d, J=8.5Hz, 4H), 7.65 (s, 2H), 7.52 (d, J=8.5Hz, 4H), 2.99 (s, 4H), 2.43 (s, 3H), 1.96 (m, J=6Hz, 8H); $^{13}$C NMR (500 MHz, $CDCl_3$) δ: 190.1, 146.4, 144.7, 141.9, 131.8, 128.2, 109.6, 57.4, 56.5, 38.2, 25.5; HRMS (ESI) m/z: 428.71 $[M+H]^+$, Microanalysis calculated for $C_{28}H_{33}N_3O$ (427.58), C: 78.65%, H: 7.78%, N: 9.83%. Found C: 78.82%, H: 7.95%, N: 10.12%.

*4.3.25. 1-Benzyl-3,5-bis-(4-pyrrolidin-1-yl-benzylidene)-piperidin-4-one* (**25**)

Light yellow crystals (2.16 g, 43%). mp: 88-89 ˚C; $^{1}$H NMR (500 MHz, $CDCl_3$) δ: 7.71 (d, J=8Hz, 2H), 7.45 (s, 2H), 7.31 (d, J=8Hz, 2H), 7.25 (d, J=7Hz, 4H), 7.19 (d, J=7Hz, 4H), 6.81 (t, J=6.5Hz, H), 4.19 (s, 2H), 2.92 (s, 4H), 1.78 (m, J=6Hz, 8H); $^{13}$C NMR (500 MHz, $CDCl_3$) δ: 192.2, 148.8, 146.3, 138.2, 137.7, 132.7, 128.5, 126.2, 125.4, 124.9, 118.9, 65.1, 58.1, 50.2, 25.7;

HRMS (ESI) m/z: 504.69 $[M+H]^+$, Microanalysis calculated for $C_{34}H_{37}N_3O$ (503.68), C: 81.08%, H: 7.40%, N: 8.34%. Found C: 81.25%, H: 7.69%, N: 8.17%.

*4.3.26. 1,5-Bis-(4-pyrrolidin-1-yl-phenyl)-penta-1,4-dien-3-one* (**26**)

Light brownish solid (2.02 g, 54%). mp: 111-113 ˚C; $^1$H NMR (500 MHz, $CDCl_3$) δ: 7.76 (d, J=6Hz, 4H), 7.52 (d, J=6Hz, 2H) , 7.12 (d, J=8Hz, 2H), 7.05 (d, J=8Hz, 4H), 1.85 (m, J=6Hz, 8H); $^{13}$C NMR (500 MHz, $CDCl_3$) δ: 190.0, 151.8, 148.2, 138.2, 136.5, 134.9, 131.2, 56.9, 26.6; HRMS (ESI) m/z: 373.82 $[M+H]^+$, Microanalysis calculated for $C_{25}H_{28}N_2O$ (372.50), C: 80.61%, H: 7.58%, N: 7.52%. Found C: 80.88%, H: 7.74%, N: 7.85%.

*4.3.27. 2,5-Bis-(4-pyrrolidin-1-yl-benzylidene)-cyclopentanone* (**27**)

Yellow powder (2.96 g, 74%). mp: 94-95 ˚C; $^1$H NMR (500 MHz, $CDCl_3$) δ: 7.87 (d, J=8Hz, 4H), 7.59 (s, 2H), 7.12 (d, J=8Hz, 4H), 2.42 (t, J=7Hz, 4H), 1.91 (m, J=6Hz, 8H); $^{13}$C NMR (500 MHz, $CDCl_3$) δ: 190.1, 149.5, 145.8, 139.1, 136.8, 134.5, 129.8, 58.1, 32.9, 26.2 ; HRMS (ESI) m/z: 399.51 $[M+H]^+$, Microanalysis calculated for $C_{27}H_{30}N_2O$ (398.54), C: 81.37%, H: 7.59%, N: 7.03%. Found C: 81.42%, H: 7.62%, N: 7.12%.

*4.3.28. 2-(4-Pyrrolidin-1-yl-benzylidene)-indan-1-one* (**28**)

White powder (1.94g, 67%). mp: 136-137 ˚C; $^1$H NMR (500 MHz, $CDCl_3$) δ: 7.94 (d, J=8Hz, 2H), 7.81 (s, H), 7.43 (d, J=8Hz, 2H), 7.37 (d, J=7.5Hz, H), 7.01 (d, J=7.5Hz, H), 6.92 (t, J=7.5Hz, H), 6.79 (t, J=7Hz, H), 2.82 (s, 2H), 1.84 (m, J=6Hz, 4H); $^{13}$C NMR (500 MHz, $CDCl_3$) δ: 192.8, 144.7, 142.9, 141.2, 139.5, 137.9, 136.6, 130.8, 129.8, 128.6, 125.2, 124.5, 122.9, 57.7, 28.5, 27.4; HRMS (ESI) m/z: 290.40 $[M+H]^+$, Microanalysis calculated for $C_{20}H_{19}NO$ (289.37), C: 83.01%, H: 6.62%, N: 4.84%. Found C: 83.25%, H: 6.75%, N: 4.82%.

*4.3.29. 2-(4-Pyrrolidin-1-yl-benzylidene)-3,4-dihydro-2H-naphthalen-1-one* (**29**)

Brown solid (2.41 g, 80%). mp: 123- 125 ˚C; $^{1}$H NMR (500 MHz, $CDCl_3$) δ: 7.76 (d, J=8Hz, 2H), 7.52 (s, H), 7.42 (d, J=8Hz, 2H), 7.21 (d, J=7.5Hz, H), 7.15 (d, J=7.5Hz, H), 7.02 (t, J=7.5Hz, H), 6.99 (t, J=7Hz, H), 2.24 (t, J=7Hz, 2H), 1.97 (t, J=7Hz, 2H), 1.81 (m, J=6Hz, 4H); $^{13}$C NMR (500 MHz, $CDCl_3$) δ: 188.8, 150.5, 149.2, 148.7, 147.4, 142.6, 135.1, 132.4, 129.8, 128.9, 125.5, 124.2, 117.5, 58.9, 29.7, 27.9, 25.9; HRMS (ESI) m/z: 304.56 $[M+H]^+$, Microanalysis calculated for $C_{21}H_{21}NO$ (303.40), C: 83.13%, H: 6.98%, N: 4.62%. Found C: 83.06%, H: 6.91%, N: 4.89%.

*4.3.30. 2-[3-(4-Pyrrolidin-1-yl-phenyl)-acryloyl]-3,4-dihydro-2H-naphthalen-1-one* (**30**)

Pale yellow solid (2.52 g, 73%). mp: 118-120 ˚C; $^{1}$H NMR (500 MHz, $CDCl_3$) δ: 7.70 (d, J=6Hz, H), 7.48 (d, J=6Hz, H), 7.33 (d, J=6.5Hz, 2H), 7.21 (d, J=6.5Hz, 2H), 7.17 (d, J=6.5Hz, H), 7.02 (d, J=6.5Hz, H), 6.98 (t, J=6.5Hz, H), 6.81 (t, J=6Hz, H), 3.24 (t, J=6Hz, H), 2.29 (t, J=8Hz, 2H), 1.98 (t, J=7Hz, 2H), 1.94 (m, J=6Hz, 4H); $^{13}$C NMR (500 MHz, $CDCl_3$) δ: 192.5, 151.8, 149.1, 145.7, 142.5, 140.4, 138.7, 136.9, 135.6, 131.9, 130.8, 129.5, 126.1, 119.1 , 65.5, 58.2, 32.5, 28.7, 25.9; HRMS (ESI) m/z: 346.57 $[M+H]^+$, Microanalysis calculated for $C_{23}H_{23}NO_2$ (345.43), C: 79.97%, H: 6.71%, N: 4.05%. Found C: 80.19%, H: 6.55%, N: 4.09%.

*4.4. DPPH (1,1-diphenyl-2-picrylhydrazyl) assay*

The reported DPPH method was applied to assess the scavenging ability of the compounds [37]. The compounds were tested in the range of 0-25 µg/mL in methanol. To 2.5 ml of compound in 5 different concentrations, 1 ml of 0.3 mM DPPH ethanol solution was added. Then 1 ml of methanol was added to the solution and allowed to react for 30 min in the dark at room temperature. The change in the absorbance was read at 518 nm. The blank was comprised of 2.5

ml of test compound and 1 ml methanol, while the mixture of 1 ml DPPH and 2.5 ml of methanol served as negative control. The percentage antioxidant activity was calculated as follows:

$$\%\ Inhibition = \frac{A_A - A_B}{A_B} \times 100$$

Where: $A_B$: absorption of blank sample, $A_A$: absorption of test samples. The $IC_{50}$ value was calculated and compared with that of ascorbic acid as a reference.

*4.5. Cell culture*

The rat pheochromocytoma (PC12) cell line was purchased from the ATCC. The cells were maintained in RPMI-1640 medium consisting of 10% heat-inactivated FBS and 1% penicillin-streptomycin. The cells were incubated at 37˚C in a 5% $CO_2$ atmosphere with 95% humidity.

*4.6. Cell viability assay*

To investigate the cytotoxicity or neuroprotective effects of synthetic compounds in PC12 cells, the MTT assay was performed. The cells ($1x10^4$cells/well) were seeded in 96-well cell culture plates and treated with different concentrations of compounds for 24 h. The cell viability was expressed as a relative percentage against control cultures. To assess the Aβ-induced neuroprotective activity, different concentrations of all compounds were individually added to cells for 24 h, before treatment with Aβ. The positive control drug selegiline was also evaluated in the same manner for comparison. 2.0 mg/ml MTT solution was added to each well and incubated for 4 h at 37°C. The medium was removed and the formazan crystals were solubilized in 100 µl dimethyl sulfoxide (DMSO). A microplate reader was used to determine the optical density (excitation at 570 nm, emission at 630 nm) and data are plotted as percent of control.

*4.7. AChE and BuChE inhibition assay*

To evaluate the potency of compounds to inhibit AChE and BuChE, all compounds were subjected to a slightly modified method of Ellman's test [38]. The reaction of released thiocholine to give a coloured product with a chromogenic reagent 5,5-dithio-bis (2-nitrobenzoic) acid (DTNB) is the basis of the spectrophotometric method. The measurements were performed on a 1700 Shimadzu UV-1700, UV-Vis spectrophotometer. At a concentration of 2.5 units/mL, the enzyme solutions were prepared in gelatin solution (1%). AChE or BChE solution (50 μL) and compound solution (50 μL), prepared in 2% DMSO at a concentration range of $10^{-1}$- $10^{-6}$ mM, were added to 3.0 mL phosphate buffer (pH 8 ± 0.1) and were incubated at 25°C for 5 min. DTNB (50 μL) and ATC (10 μL) were added to the enzyme-inhibitor mixture to start the reaction. For 10 min, the production of the yellow anion was recorded at 412 nm. Serving as a control, an identical solution of the enzyme without the inhibitor was processed using the same protocol. The blank reading consisted of 3.0 mL buffer, 50 μL 2% DMSO, 50 μL DTNB and 10 μL substrate. All the processes were assayed in triplicate. The percentage inhibition rate was calculated by the following equation:

$$\%\, Inhibition = \frac{A_C - A_I}{A_C} \times 100$$

Where $A_I$ is the absorbance in the presence of the inhibitor, $A_C$ is the absorbance of the control and $A_B$ is the absorbance of blank. Both values were corrected with blank-reading value. The data was expressed as Mean ± SD.

*4.8. Molecular docking and QSAR analysis*

For docking, the molecules were drawn using ACD Chemsketch 12 freeware followed by energy optimization using MMFF94 force field in TINKER [32]. The protein was first subjected to energy minimization, protonation followed by detection of site detection. The receptor and the drug candidates were optimized before actual docking followed by docking in MOE using the

standard procedure found in the manual of software. The molecules were docked in the active site using 'force field' as a refinement technique with default settings in MOE [29]. All of the newly synthesized molecules were docked in the active site of AChE (pdb- 1GQR, x-ray resolution = 2.20 $A^o$). For the sake of convenience and comparison, as a representative, we report the docking poses for the most active compound of the series. For QSAR analysis, e-Dragon was used to calculate myriad number of descriptors, followed by random splitting of dataset into training set (80%) and test set (20%). QSARINS v1.2 was used to eliminate redundant descriptors and for building GA-MLR (Genetic Algorithm-Multilinear regression) model [31, 32].

**ACKNOWLEDGMENTS**

SNAB thanks University Kebangsaan Malaysia for post-doctoral contract and highly obliged to Professor Dr. David Schubert, Head of cellular neurobiology laboratory, Salk Institute (USA), for his kind suggestions and reading the manuscript. VHM is thankful to Dr. Paola Gramatica, Italy for providing evaluation copy of QSARINS and to NCL, Pune for allowing to perform the computational work. Authors gratefully acknowledge the generous support provided by the University Kebangsaan Malaysia (UKM-DLP-2013-013).

**REFERENCES**

[1] World Alzheimer Report 2013 Alzheimer's Disease International, (2013) 1.

[2] D.K. Lahiri, M.R. Farlow, N.H. Greig, K. Sambamurti, Current drug targets for Alzheimer's disease treatment, Drug Dev Res, 56 (2002) 267-281.

[3] J.L. Cummings, Alzheimer's Disease, N Engl J Med, 351 (2004) 56-67.

[4] J.A. Bailey, D.K. Lahiri, A novel effect of rivastigmine on pre-synaptic proteins and neuronal viability in a neurodegeneration model of fetal rat primary cortical cultures and its implication in Alzheimer's disease, J Neurochem, 112 (2010) 843-853.

[5] A. Enz, R. Amstutz, H. Boddeke, G. Gmelin, J. Malanowski, Brain selective inhibition of acetylcholinesterase: a novel approach to therapy for Alzheimer's disease, Prog Brain Res, 98 (1993) 431-438.

[6] E. Giacobini, Cholinesterase inhibitors: new roles and therapeutic alternatives, Pharmacol Res, 50 (2004) 433-440.

[7] P.J. Houghton, Y. Ren, M.-J. Howes, Acetylcholinesterase inhibitors from plants and fungi, Nat Prod Rep, 23 (2006) 181-199.

[8] N.H. Greig, T. Utsuki, Q.-s. Yu, X. Zhu, H.W. Holloway, T. Perry, B. Lee, D.K. Ingram, D.K. Lahiri, A New Therapeutic Target in Alzheimer's Disease Treatment: Attention to Butyrylcholinesterase, Curr Med Res Opin, 17 (2001) 159-165.

[9] J. Lal, S.K. Gupta, D. Thavaselvam, D.D. Agarwal, Design, synthesis, synergistic antimicrobial activity and cytotoxicity of 4-aryl substituted 3,4-dihydropyrimidinones of curcumin, Bioorg Med Chem Lett, 22 (2012) 2872-2876.

[10] A.M. Magerramov, M.M. Kurbanova, R.T. Abdinbekova, I.A. Rzaeva, V.M. Farzaliev, M.A. Allakhverdiev, Synthesis and antioxidative properties of some 3,4-dihydropyrimidin-2(1H)ones (-thiones), Russ J Appl Chem, 79 (2006) 787-790.

[11] R. Feng, Y. Lu, L.L. Bowman, Y. Qian, V. Castranova, M. Ding, Inhibition of Activator Protein-1, NF-κB, and MAPKs and Induction of Phase 2 Detoxifying Enzyme Activity by Chlorogenic Acid, J Biol Chem, 280 (2005) 27888-27895.

[12] S.N.A. Bukhari, Y. Tajuddin, V.J. Benedict, K.W. Lam, I. Jantan, J. Jalil, M. Jasamai, Synthesis and Evaluation of Chalcone Derivatives as Inhibitors of Neutrophils' Chemotaxis, Phagocytosis and Production of Reactive Oxygen Species, Chem Biol Drug Des, 83 (2014) 198-206.

[13] S.N. Bukhari, I. Jantan, M. Jasamai, Anti-inflammatory trends of 1, 3-diphenyl-2-propen-1-one derivatives, Mini Rev Med Chem, 13 (2013) 87-94.

[14] S.N. Bukhari, M. Jasamai, I. Jantan, Synthesis and biological evaluation of chalcone derivatives (mini review), Mini Rev Med Chem, 12 (2012) 1394-1403.

[15] S. Bag, S. Ghosh, R. Tulsan, A. Sood, W. Zhou, C. Schifone, M. Foster, H. LeVine Iii, B. Török, M. Török, Design, synthesis and biological activity of multifunctional α,β-unsaturated carbonyl scaffolds for Alzheimer's disease, Bioorg Med Chem Lett, 23 (2013) 2614-2618.

[16] D. Silva, M. Chioua, A. Samadi, P. Agostinho, P. Garção, R. Lajarín-Cuesta, C. de los Ríos, I. Iriepa, I. Moraleda, L. Gonzalez-Lafuente, E. Mendes, C. Pérez, M.I. Rodríguez-Franco, J. Marco-Contelles, M. Carmo Carreiras, Synthesis, Pharmacological Assessment, and Molecular Modeling of Acetylcholinesterase/Butyrylcholinesterase Inhibitors: Effect against Amyloid-β-Induced Neurotoxicity, ACS Chem Neurosci, 4 (2013) 547-565.

[17] R. Sultana, M. Perluigi, D.A. Butterfield, Oxidatively modified proteins in Alzheimer's disease (AD), mild cognitive impairment and animal models of AD: role of Abeta in pathogenesis, Acta Neuropathol, 118 (2009) 131-150.

[18] X. Zhu, B. Su, X. Wang, M.A. Smith, G. Perry, Causes of oxidative stress in Alzheimer disease, Experientia, 64 (2007) 2202-2210.

[19] R.J. Mark, M.A. Lovell, W.R. Markesbery, K. Uchida, M.P. Mattson, A Role for 4-Hydroxynonenal, an Aldehydic Product of Lipid Peroxidation, in Disruption of Ion Homeostasis and Neuronal Death Induced by Amyloid β-Peptide, J Neurochem, 68 (1997) 255-264.

[20] D.A. Butterfield, K. Hensley, M. Harris, M. Mattson, J. Carney, β-Amyloid Peptide Free Radical Fragments Initiate Synaptosomal Lipoperoxidation in a Sequence-Specific Fashion: Implications to Alzheimer′s Disease, Biochem Biophys Res Commun, 200 (1994) 710-715.

[21] S.N. Bukhari, I. Jantan, O.U. Tan, M. Sher, N.U. Hassan, H.L. Qin, Biological Activity and Molecular Docking Studies of Curcumin Related alpha, beta- Unsaturated Carbonyl Based Synthetic Compounds as Anticancer Agents and Mushroom Tyrosinase Inhibitors, J Agric Food Chem, (2014) In Press.

[22] S.N.A. Bukhari, G. Lauro, I. Jantan, G. Bifulco, M.W. Amjad, Pharmacological Evaluation and Docking Studies of α, β-Unsaturated Carbonyl Based Synthetic Compounds as Inhibitors of Secretory Phospholipase A2, Cyclooxygenases, Lipoxygenase and Proinflammatory Cytokines, Bioorg Med Chem, (2014) In Press.

[23] J.R. Dimmock, M.P. Padmanilayam, R.N. Puthucode, A.J. Nazarali, N.L. Motaganahalli, G.A. Zello, J.W. Quail, E.O. Oloo, H.-B. Kraatz, J.S. Prisciak, T.M. Allen, C.L. Santos, J. Balzarini, E. De Clercq, E.K. Manavathu, A Conformational and Structure−Activity Relationship

Study of Cytotoxic 3,5-Bis(arylidene)-4-piperidones and Related N-Acryloyl Analogues, J Med Chem, 44 (2001) 586-593.

[24] U. Das, M. Kawase, H. Sakagami, A. Ideo, J. Shimada, J. Molnár, Z. Baráth, Z. Bata, J.R. Dimmock, 3-(3,4,5-Trimethoxyphenyl)-1-oxo-2-propene: A novel pharmacophore displaying potent multidrug resistance reversal and selective cytotoxicity, Bioorg Med Chem, 15 (2007) 3373-3380.

[25] U. Das, J. Alcorn, A. Shrivastav, R.K. Sharma, E. De Clercq, J. Balzarini, J.R. Dimmock, Design, synthesis and cytotoxic properties of novel 1-[4-(2-alkylaminoethoxy)phenylcarbonyl]-3,5-bis(arylidene)-4-piperidones and related compounds, Eur J Med Chem, 42 (2007) 71-80.

[26] Y. Kia, H. Osman, R.S. Kumar, V. Murugaiyah, A. Basiri, S. Perumal, H.A. Wahab, C.S. Bing, Synthesis and discovery of novel piperidone-grafted mono- and bis-spirooxindole-hexahydropyrrolizines as potent cholinesterase inhibitors, Bioorg Med Chem, 21 (2013) 1696-1707.

[27] J.-M. Contreras, Y.M. Rival, S. Chayer, J.-J. Bourguignon, C.G. Wermuth, Aminopyridazines as Acetylcholinesterase Inhibitors, J Med Chem, 42 (1999) 730-741.

[28] K.K. Roy, A. Dixit, A.K. Saxena, An investigation of structurally diverse carbamates for acetylcholinesterase (AChE) inhibition using 3D-QSAR analysis, J Mol Graph Model, 27 (2008) 197-208.

[29] Y.K. Yoon, M.A. Ali, A.C. Wei, T.S. Choon, K.-Y. Khaw, V. Murugaiyah, H. Osman, V.H. Masand, Synthesis, characterization, and molecular docking analysis of novel benzimidazole derivatives as cholinesterase inhibitors, Bioorg Chem, 49 (2013) 33-39.

[30] D. Mahajan, V. Masand, K. Patil, T. Hadda, V. Rastija, Integrating GUSAR and QSAR analyses for antimalarial activity of synthetic prodiginines against multi drug resistant strain, Med Chem Res, 22 (2013) 2284-2292.

[31] V.H. Masand, D.T. Mahajan, K.N. Patil, T.B. Hadda, M.H. Youssoufi, R.D. Jawarkar, I.G. Shibi, Optimization of antimalarial activity of synthetic prodiginines: QSAR, GUSAR, and CoMFA analyses, Chem Biol Drug Des, 81 (2013) 527-536.

[32] V. Masand, D. Mahajan, T. Hadda, R. Jawarkar, H. Chavan, B.P. Bandgar, H. Chauhan, Molecular docking and quantitative structure–activity relationship (QSAR) analyses of indolylarylsulfones as HIV-1 non-nucleoside reverse transcriptase inhibitors, Med Chem Res, 23 (2014) 417-425.

[33] D.T. Mahajan, V.H. Masand, K.N. Patil, T. Ben Hadda, R.D. Jawarkar, S.D. Thakur, V. Rastija, CoMSIA and POM analyses of anti-malarial activity of synthetic prodiginines, Bioorg Med Chem Lett, 22 (2012) 4827-4835.

[34] P. Gramatica, On the development and validation of QSAR models, Methods Mol Biol, 930 (2013) 499-526.

[35] P. Gramatica, N. Chirico, E. Papa, S. Cassani, S. Kovarich, QSARINS: A new software for the development, analysis, and validation of QSAR MLR models, J Comput Chem, 34 (2013) 2121-2132.

[36] G.L. Ellman, K.D. Courtney, V. Andres jr, R.M. Featherstone, A new and rapid colorimetric determination of acetylcholinesterase activity, Biochem Pharmacol, 7 (1961) 88-95.

[37] C.W. Choi, S.C. Kim, S.S. Hwang, B.K. Choi, H.J. Ahn, M.Y. Lee, S.H. Park, S.K. Kim, Antioxidant activity and free radical scavenging capacity between Korean medicinal plants and flavonoids by assay-guided comparison, Plant Sci, 163 (2002) 1161-1168.

[38] N.S. Perry, P.J. Houghton, A. Theobald, P. Jenner, E.K. Perry, In-vitro inhibition of human erythrocyte acetylcholinesterase by salvia lavandulaefolia essential oil and constituent terpenes, J Pharm Pharmacol, 52 (2000) 895-902.

## Captions

**Scheme 1:** Structures and synthesis scheme of α, β-unsaturated carbonyl based compounds. Reagents and conditions: (i) NaOH, EtOH, Room temperature.

**Table 1:** Antioxidant activity and inhibitory effects of synthetic α, β-unsaturated carbonyl based compounds against AChE and BChE.

**Figure 1**: Protective effects of the most active synthetic compounds against $A\beta_{1-42}$-induced cell damage. Cell viability of compounds was evaluated using the MTT assay. All groups were treated with 25 μM $A\beta_{1-42}$ except for the control group. Selegiline was used as a positive control at the same concentrations. Synthetic compounds and selegiline were pre-incubated at various concentrations (0.01-100 μM) in serum-free media for 24 h before the addition of Aβ peptide. Cell viability is expressed as the mean percentage of viable cells compared with the untreated cells. The data are the mean ± SE (n=5).

**Figure 2:** Docking pose for most active molecule **4** in the active site of AChE

**Figure 3:** Docking pose for most active molecule **4** with surface area of active site of AChE.

**Figure 4:** Correlation between experimental and predicted $pIC_{50}$

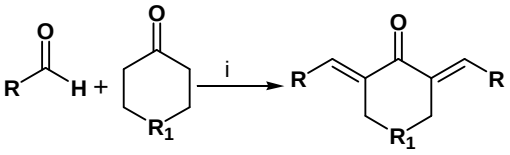


| | R | $R_1$ |
|---|---|---|
| **1** | 4-Diethoxymethyl-benzene | $CH_2$ |
| **2** | 4-Diethoxymethyl-benzene | O |
| **3** | 4-Diethoxymethyl-benzene | NH |
| **4** | 4-Diethoxymethyl-benzene | $NCH_3$ |
| **5** | 4-Diethoxymethyl-benzene | $NCH_2$-benzene |
| **11** | Phenyl-2-nitro-4-dimethylamine | $CH_2$ |
| **12** | Phenyl-2-nitro-4-dimethylamine | O |
| **13** | Phenyl-2-nitro-4-dimethylamine | NH |
| **14** | Phenyl-2-nitro-4-dimethylamine | $NCH_3$ |
| **15** | Phenyl-2-nitro-4-dimethylamine | $NCH_2$-benzene |
| **21** | Phenyl-4-pyrrolidine | $CH_2$ |
| **22** | Phenyl-4-pyrrolidine | O |
| **23** | Phenyl-4-pyrrolidine | NH |
| **24** | Phenyl-4-pyrrolidine | $NCH_3$ |
| **25** | Phenyl-4-pyrrolidine | $NCH_2$-benzene |

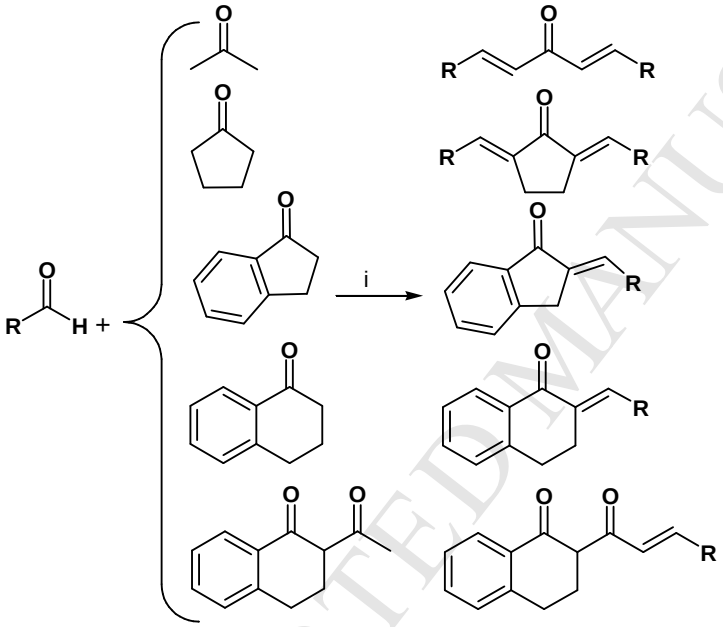


| R | |
|---|---|
| **6** | 4-Diethoxymethyl-benzene |
| **16** | Phenyl-2-nitro-4-dimethylamine |
| **26** | Phenyl-4-pyrrolidine |
| **7** | 4-Diethoxymethyl-benzene |
| **17** | Phenyl-2-nitro-4-dimethylamine |
| **27** | Phenyl-4-pyrrolidine |
| **8** | 4-Diethoxymethyl-benzene |
| **18** | Phenyl-2-nitro-4-dimethylamine |
| **28** | Phenyl-4-pyrrolidine |
| **9** | 4-Diethoxymethyl-benzene |
| **19** | Phenyl-2-nitro-4-dimethylamine |
| **29** | Phenyl-4-pyrrolidine |
| **10** | 4-Diethoxymethyl-benzene |
| **20** | Phenyl-2-nitro-4-dimethylamine |
| **30** | Phenyl-4-pyrrolidine |

**Scheme 1:** Structures and synthesis scheme of α, β-unsaturated carbonyl based compounds. Reagents and conditions: (i) NaOH, EtOH, Room temperature.

**Table 1:** Antioxidant activity and inhibitory effects of synthetic α, β-unsaturated carbonyl based compounds against AChE and BChE.

| Compounds | $IC_{50}$ AChE (μM) | $IC_{50}$ BuChE (μM) | Selectivity for AChE[a] | $IC_{50}$ DPPH (μM) |
|---|---|---|---|---|
| **1** | 12.43±1.22 | 43.66±1.93 | 3.51 | 20.12±1.20 |
| **2** | 41.22±2.20 | 38.53±1.64 | 0.93 | 29.30±1.83 |
| **3** | 0.92±0.73 | 12.34±0.67 | 13.41 | 19.29±3.20 |
| **4** | 0.042±0.01 | >100 | - | 20.40±1.93 |
| **5** | 27.54±2.21 | 65.27±0.52 | 2.37 | 28.22±0.96 |
| **6** | 55.34±1.76 | 88.93±2.37 | 1.61 | >50 |
| **7** | 76.64±3.21 | 14.66±0.68 | 0.19 | >50 |
| **8** | >100 | >100 | - | 37.22±2.54 |
| **9** | >100 | >100 | - | 39.45±5.44 |
| **10** | 76.93±1.89 | >100 | - | >50 |
| **11** | 45.29±2.71 | >100 | - | 32.46±2.16 |
| **12** | 1.54±0.02 | 19.74±1.22 | 12.82 | 29.22±1.34 |
| **13** | 0.88±0.04 | 22.65±1.28 | 25.74 | 25.67±0.45 |
| **14** | 0.057±0.05 | >100 | - | 18.39±1.75 |
| **15** | >100 | >100 | - | >50 |
| **16** | >100 | >100 | - | >50 |
| **17** | >100 | >100 | - | 47.77±4.27 |
| **18** | >100 | >100 | - | >50 |
| **19** | 79.31±2.84 | >100 | - | 22.99±2.14 |
| **20** | 39.44±1.73 | >100 | - | 49.10±1.76 |

| | | | | |
|---|---|---|---|---|
| **21** | >100 | >100 | - | 31.29±2.43 |
| **22** | >100 | >100 | - | >50 |
| **23** | 9.52±0.45 | >100 | - | 26.94±0.85 |
| **24** | 2.78±0.55 | 66.75±5.76 | 24.01 | 43.28±1.48 |
| **25** | >100 | 56.92±2.87 | - | >50 |
| **26** | >100 | >100 | - | >50 |
| **27** | 66.43±2.91 | >100 | - | >50 |
| **28** | >100 | >100 | - | >50 |
| **29** | >100 | >100 | - | 29.22±1.67 |
| **30** | >100 | >100 | - | 27.87±2.51 |
| **Donepezil** | 0.062±0.08 | 6.92±0.21 | 111.61 | - |
| **Ascorbic acid** | - | - | - | 19.36±1.55 |

[a]AChE selectivity index defined as $IC_{50}$ BChE/$IC_{50}$ AChE affinity ratio.

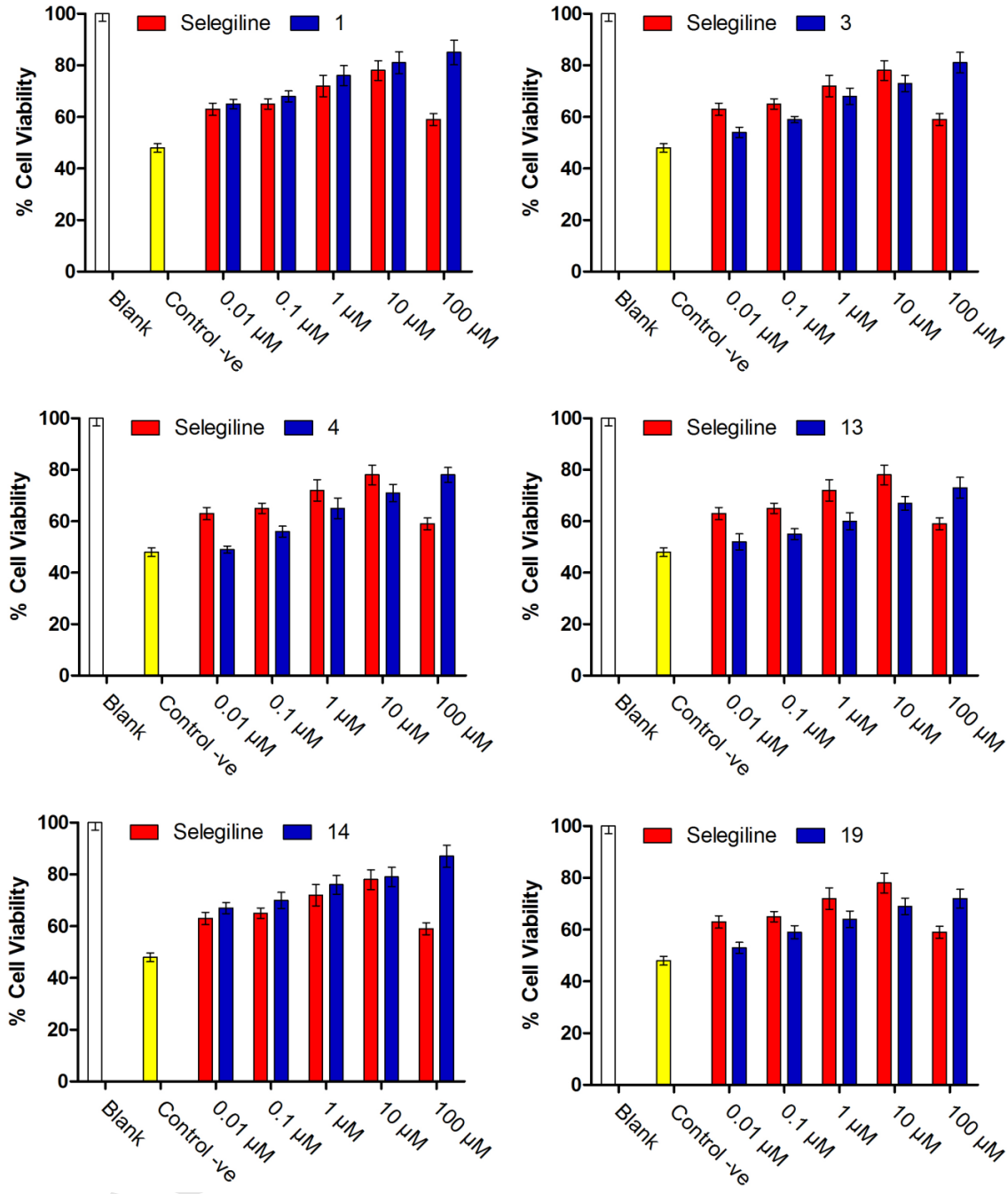


**Figure 1**: Protective effects of the most active synthetic compounds against $A\beta_{1-42}$-induced cell damage. Cell viability of compounds was evaluated using the MTT assay. All groups were treated with 25 µM $A\beta_{1-42}$ except for the control group. Selegiline was used as a positive control at the same concentrations. Synthetic compounds and selegiline were pre-incubated at various concentrations (0.01-100 µM) in serum-free media for 24 h before the addition of Aβ peptide. Cell viability is expressed as the mean percentage of viable cells compared with the untreated cells. The data are the mean ± SE (n=5).

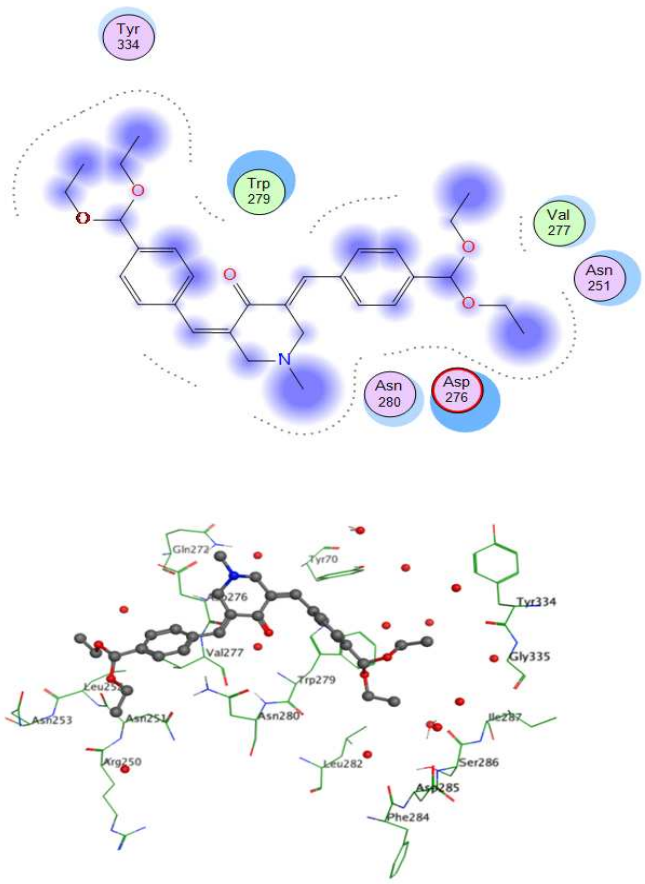


**Figure 2:** Docking pose for most active molecule **4** in the active site of AChE

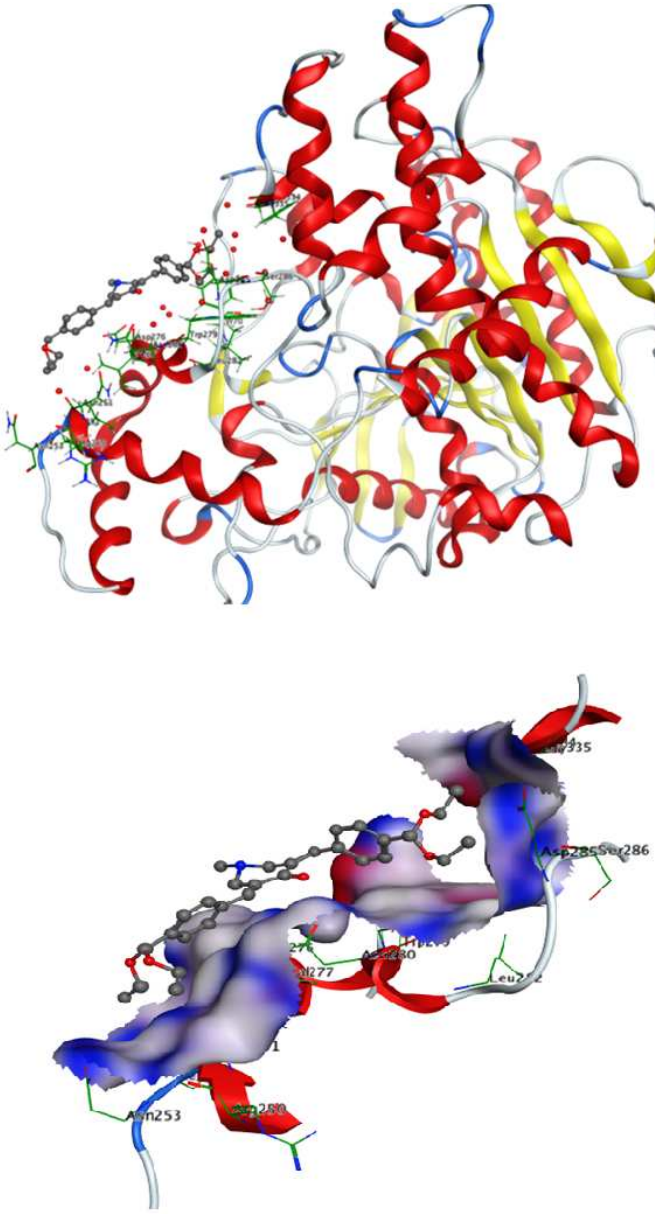


**Figure 3:** Docking pose for most active molecule **4** with surface area of active site of AChE.

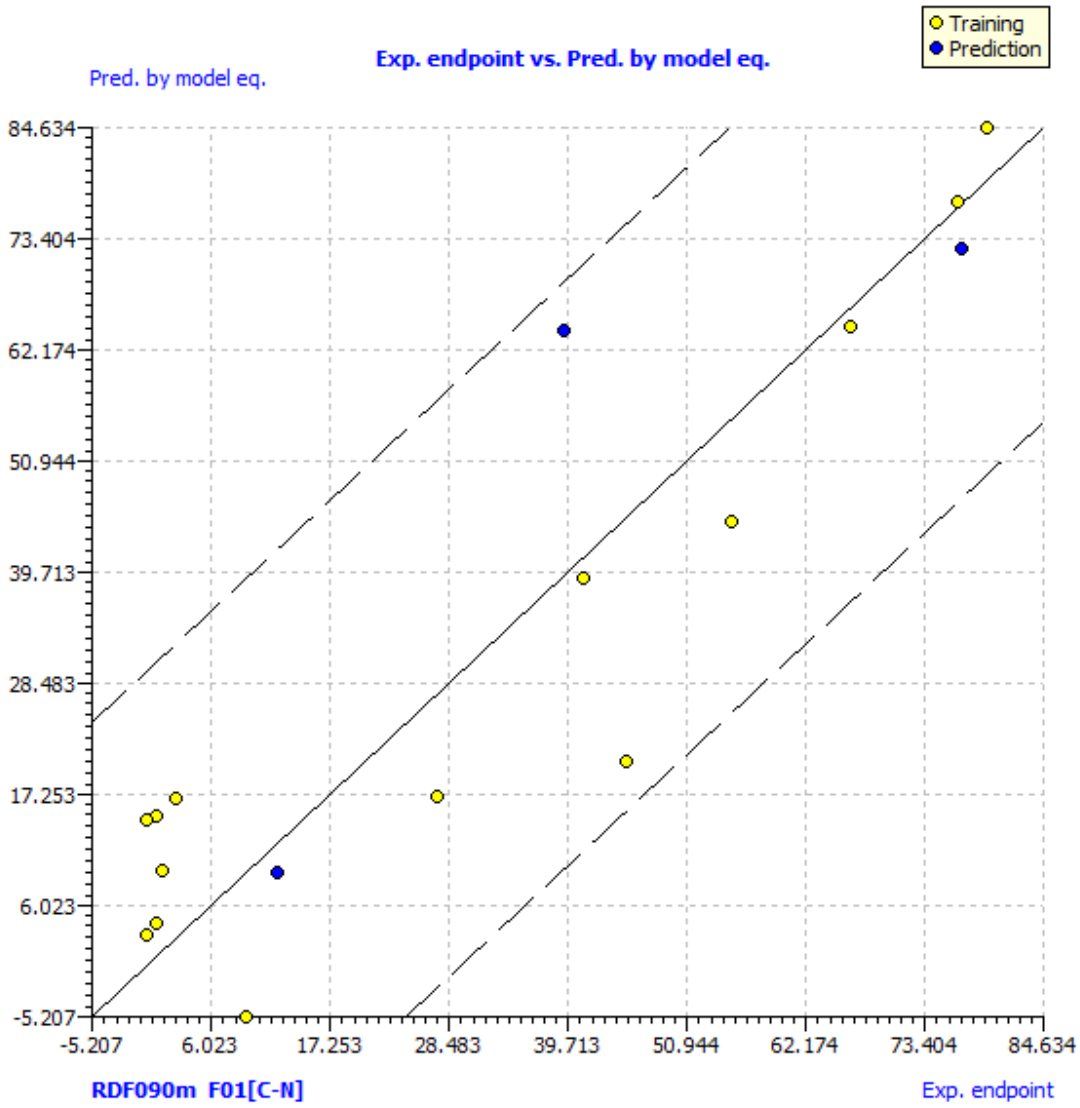


**Figure 4:** Correlation between experimental and predicted $pIC_{50}$

# Supplementary material

**Synthesis of α, β-Unsaturated Carbonyl Based Compounds as Acetylcholinesterase and Butyrylcholinesterase Inhibitors: Characterization, Molecular Modeling, QSAR Studies and Effect Against Amyloid β-Induced Cytotoxicity**

Syed Nasir Abbas Bukhari[a]*, Ibrahim Jantan[a]*, Vijay H. Masand[b], Devidas T. Mahajan[b,] Muhammad Sher[c], M.Naeem-ul-Hassan[c], Muhammad Wahab Amjad[a], Oya Unsal Tan[d]

a. *Drug and Herbal Research Centre, Faculty of Pharmacy, Universiti Kebangsaan Malaysia, Jalan Raja Muda Abdul Aziz, 50300 Kuala Lumpur, Malaysia*
b. *Department of Chemistry, Vidya Bharati Mahavidyalaya, Amravati, Maharashtra, India- 444 602.*
c. *Department of Chemistry, University of Sargodha, Sargodha 40100, Pakistan.*
*d. Department of Pharmaceutical Chemistry, Faculty of Pharmacy, Hacettepe University, Ankara 06100, Turkey*

***** Authors to whom correspondence should be addressed;

E mail: (SNAB) snab@pharmacy.ukm.my; snab_hussaini@yahoo.com

(IJ) ibj@pharmacy.ukm.my

Tel: +6-01123695295

Fax: +6-0326983271

**Table of contents:**

$^{1}$H NMR and $^{13}$C NMR spectra of α, β-Unsaturated Carbonyl Based Compounds

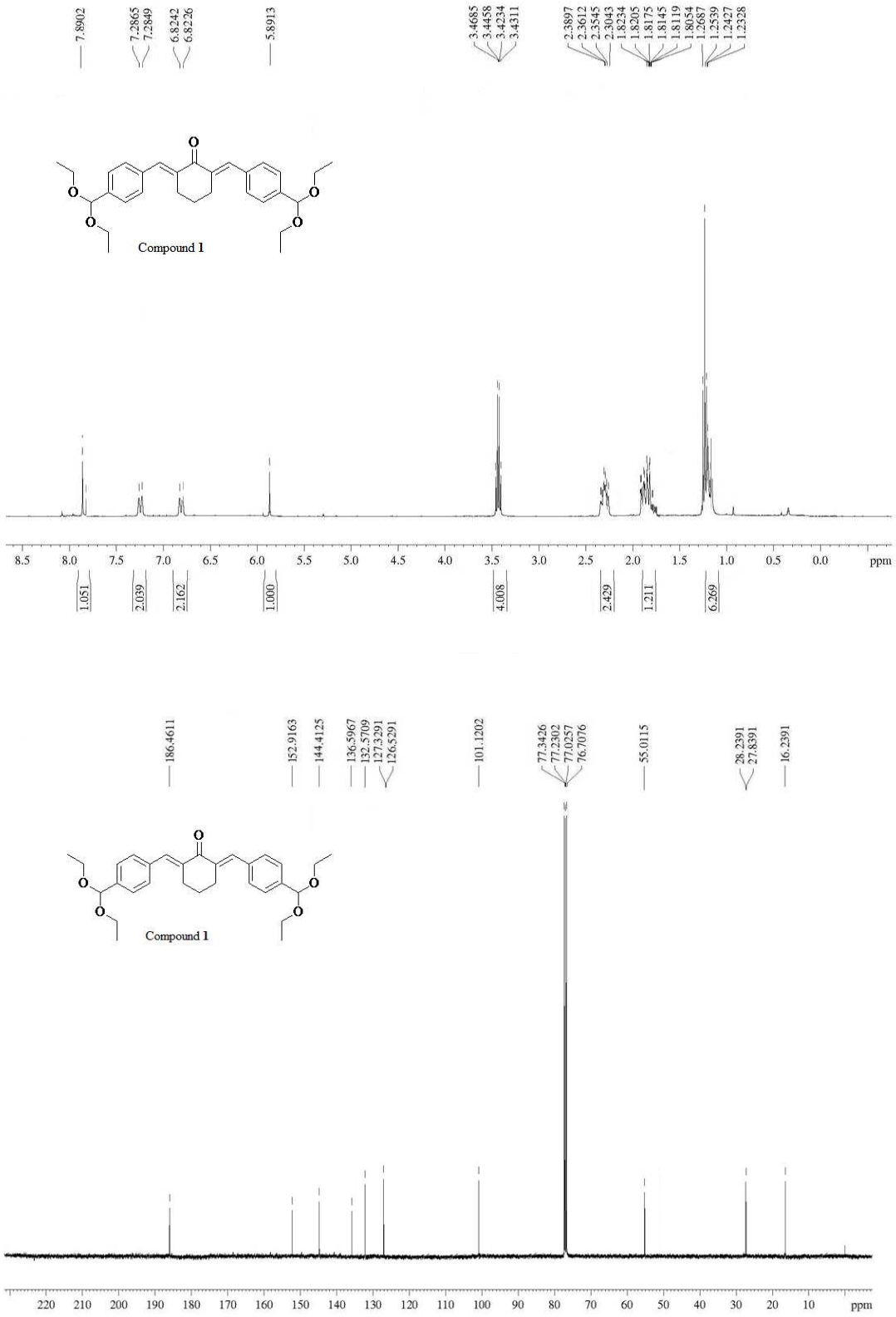


$^{1}$H NMR and $^{13}$C NMR spectra of compound **1**

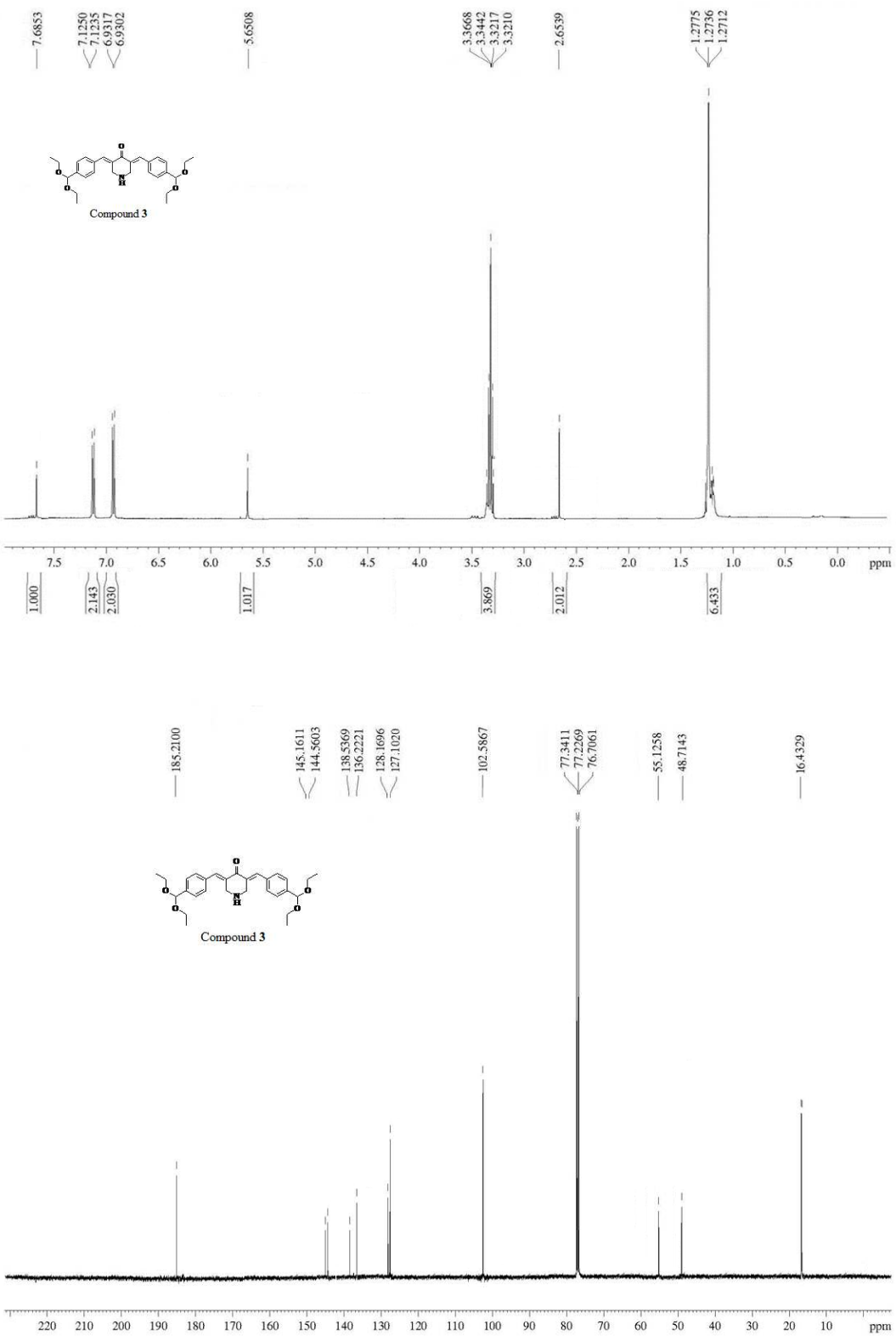


$^{1}$H NMR and $^{13}$C NMR spectra of compound **3**

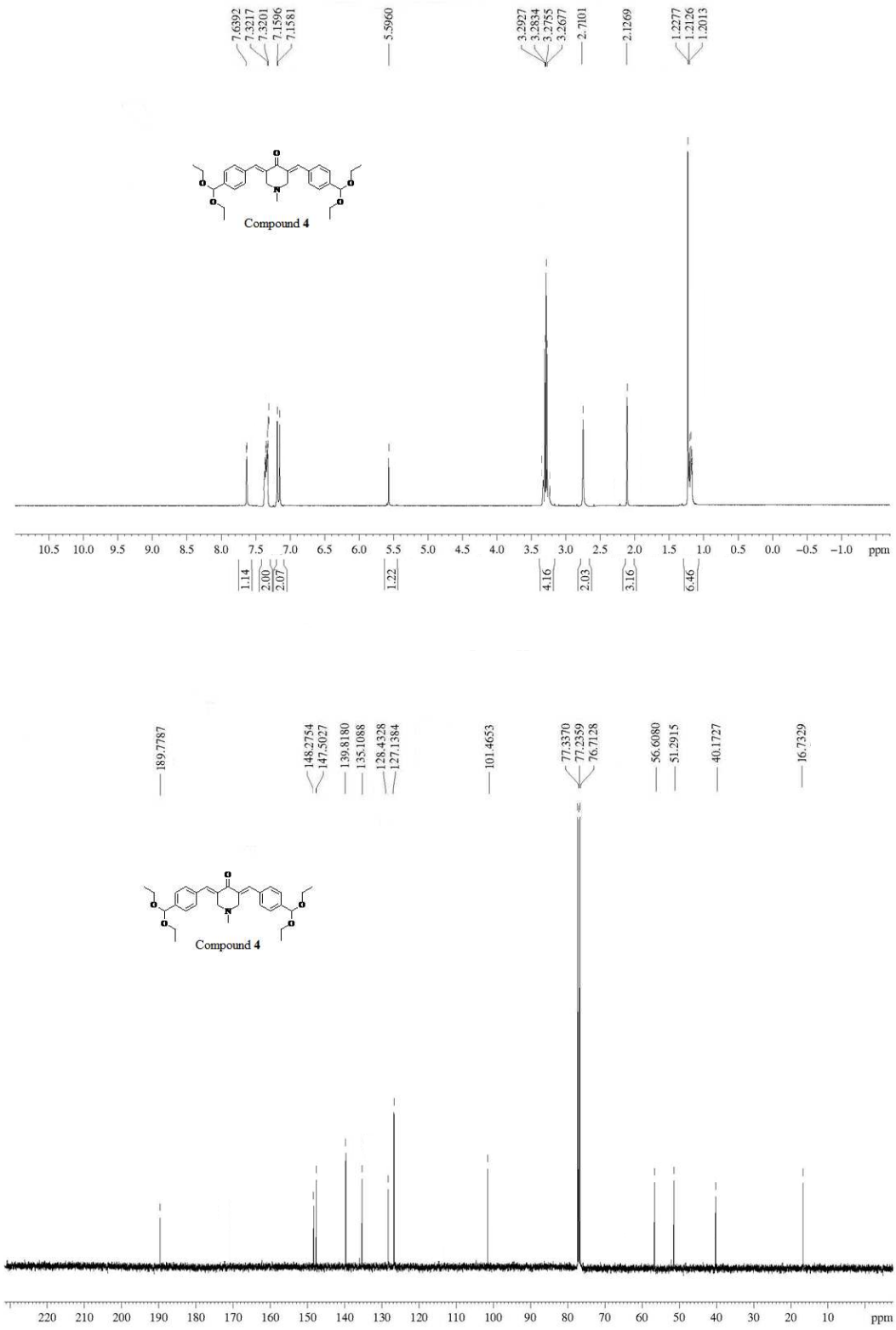


$^{1}$H NMR and $^{13}$C NMR spectra of compound **4**

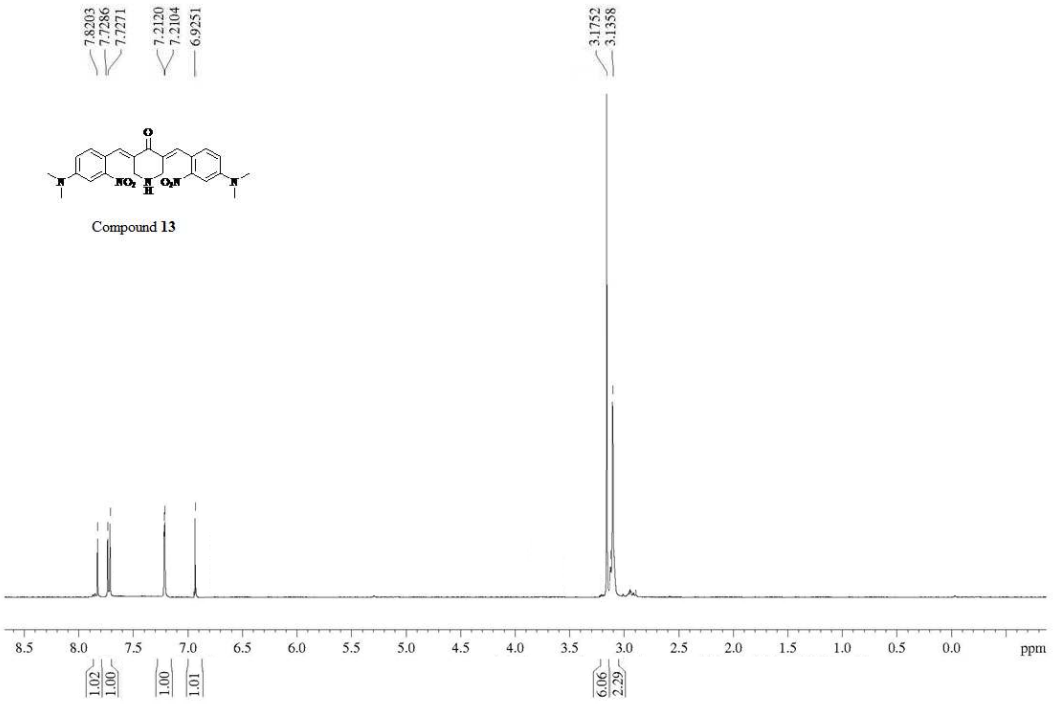


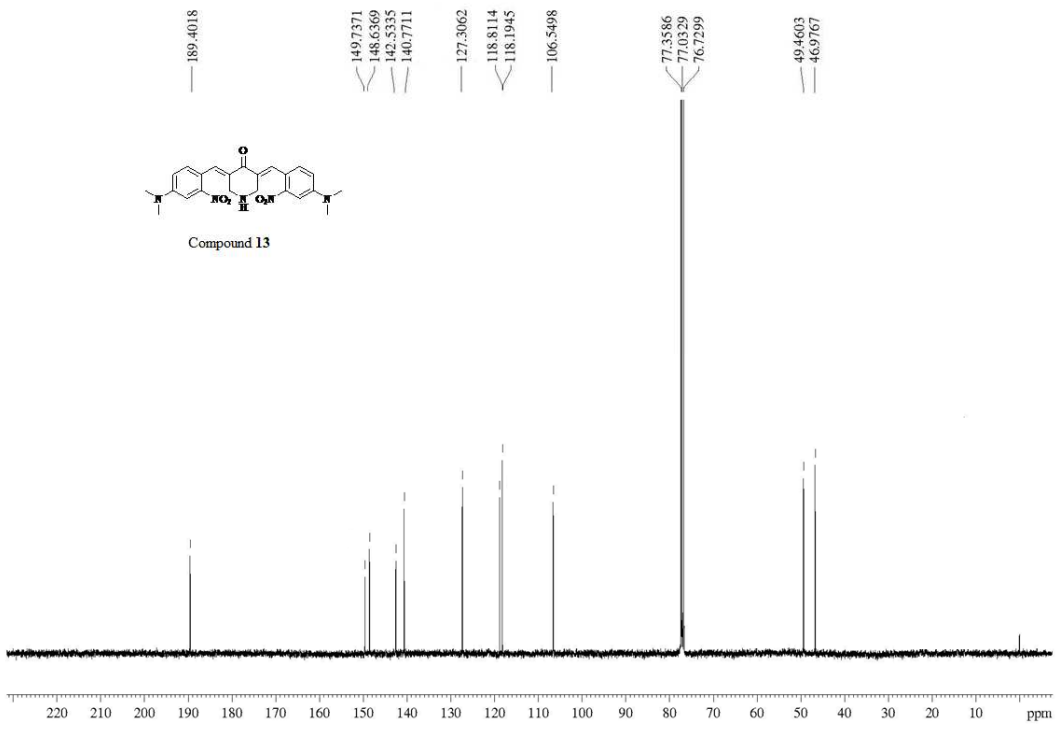


$^{1}$H NMR and $^{13}$C NMR spectra of compound **13**

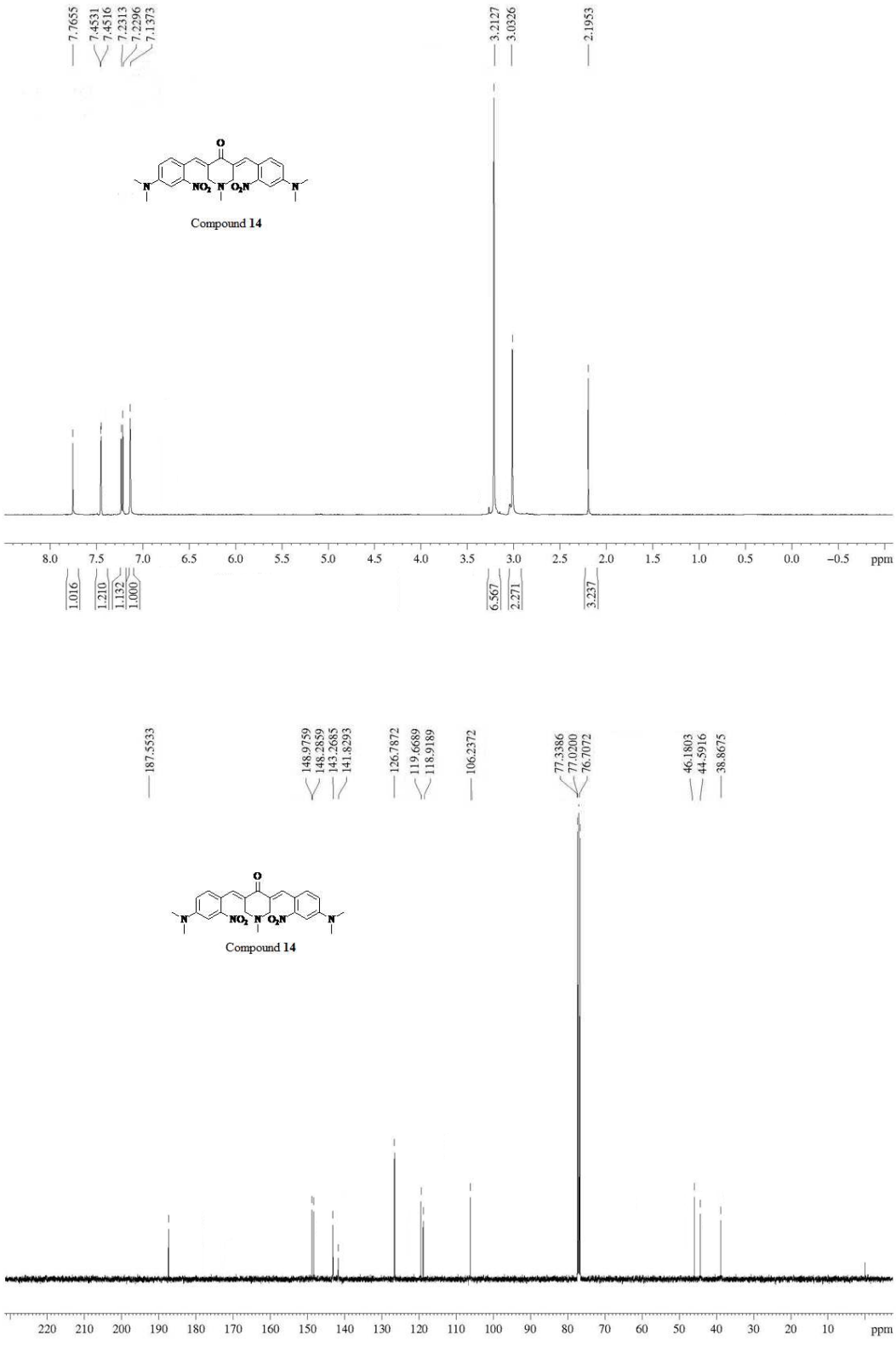


$^{1}$H NMR and $^{13}$C NMR spectra of compound **14**